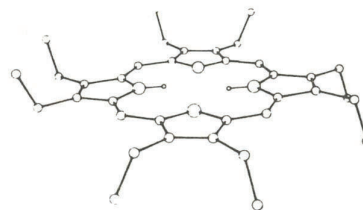


PHOTOCHEMICAL HOLE-BURNING
IN ORGANIC SOLIDS AT LOW TEMPERATURE



20 oktober 1987
doctoraalscriptie
ARNOUD VISSER

PHOTOCHEMICAL HOLE-BURNING
IN ORGANIC SOLIDS AT LOW TEMPERATURE

The work presented in this report was performed by Arnoud Visser in the group "Moleculen in Aangeslagen Toestand" of Prof. J.H. van der Waals and Prof. J. Schmidt. The study was carried out under the supervision of Dr. S. Völker between March 1986 and October 1987.

CONTENTS.

INTRODUCTION.

CHAPTER 1. HIGH RESOLUTION SPECTROSCOPY OF OCTAETHYLPORPHIN AN ITS α -CHLORO DERIVATIVE IN CRYSTALLINE AND GLASSY HOST AT 4.2 K.

1. Introduction.
2. Experimental.
3. Results and discussion.
 - 3.1 Octaethylporphin.
 - 3.2 α -chloro-octaethylporphin .
 - 3.3 Comparison of OEP, α -Cl-OEP and various free-base porphins.
4. Conclusion

CHAPTER 2. OPTICAL DEPHASING OF THE $S_1 + S_0$ TRANSITION OF FREEBASE OCTAETHYLPORPHIN IN N-OCTANE AND POLYSTERENE STUDIED BY PHOTOCHEMICAL HOLE-BURNING.

1. Introduction.
2. Experimental.
3. Results and discussion.
 - 3.1 Temperature dependence of the 0-0 transition of OEP in crystalline n-octane.
 - 3.2 Temperature dependence of the 0-0 transition of OEP in amorphous polysterene.

CHAPTER 3. SPECTRAL HOLEBURNING IN ORGANIC GLASSES.
A STUDY OF RESORUFIN AND FREE-BASE PORPHIN BETWEEN 0.3 AND 20 K.

1. Introduction.
2. Experimental.
3. Results and discussion.
4. Conclusions.

INTRODUCTION

In this report a high resolution spectroscopy and hole-burning study of electronically excited singlet states of four organic molecules incorporated in various organic hosts is presented. Three of these molecules are closely related to each other: free-base porphyrin (H_2P) and its derivatives octaethylporphyrin (OEP) and α -chloro-octaethylporphyrin (α -Cl-OEP). Porphyrin molecules are interesting because their derivatives play an important function in redox processes in nature. For example, the heme group in hemoglobin and cytochrome is an iron porphyrin, and chlorophyll is a derivative of magnesium chlorin, the reduced form of H_2P . The optical properties of these biological molecules are largely determined by the porphyrin nucleus. The fourth molecule is the ionic dye resorufin.

The first chapter of this report deals with the spectroscopy of OEP and α -Cl-OEP as guests in n-octane crystals and 2-methyl-tetrahydrofuran (MTHF) glass at 4.2 K. We have observed that these systems undergo the same phototautomeric reaction as H_2P , namely that the inner protons switch from one pair of opposite nitrogens to the other by selective irradiation with laser light. We have made use of this hole-burning process and combined it with site-selective spectroscopy to determine the vibrational frequencies of the ground state S_0 and first excited singlet state S_1 of these two porphyrin derivatives, which were not known so far. Furthermore we tried to identify the second excited singlet state S_2 of OEP. Doubts about the spectral position, however, remain. At high concentrations of OEP in MTHF we have observed new spectral bands at $\sim 600\text{ cm}^{-1}$ to the low energy side of the 0-0 band, which we attribute to a dimer of OEP.

In the second chapter we present a hole-burning study of optical dephasing of the S_1+S_0 0-0 transition of OEP in free sites of n-octane and in the polymer polystyrene. In the crystalline n-octane we found an exponential temperature dependence of the homogeneous linewidth, similar to what has been observed in organic mixed crystals. The activation energies measured were

smaller than 10 cm^{-1} , which we have interpreted as a librational mode of the OEP molecule which has a very loose fit in the host. In the polystyrene polymer we found a $T^{1.3}$ dependence of the homogeneous linewidth between 1.2 and 4.2 K, as already earlier reported in the literature, but the absolute values of our linewidths were reduced by a factor of ~ 1.5 in comparison to those. We are planning measurements on these systems over a wider temperature regime in order to understand their dynamical behaviour in a quantitative manner.

In the last chapter a study is reported on the temperature dependence of holes burnt in the $S_1 + S_0$ 0-0 transition of resorufin and H_2P in various organic amorphous hosts between ~ 0.3 and ~ 20 K. A $T^{1.3}$ dependence is found over almost two decades in temperature, which is in contrast with recently reported photon echo and hole-burning results. Our data have been fitted with a theoretical model. A discussion of our results on resorufin in glycerol is given and compared with photon echo and hole-burning data of the literature.

HIGH RESOLUTION SPECTROSCOPY OF OCTAETHYLPORPHIN AND ITS
 α -CHLORO DERIVATIVE IN CRYSTALLINE AND GLASSY HOSTS AT 4.2 K.

A. Visser and S. Völker

ABSTRACT

Site-selection spectroscopy and photochemical hole-burning have been used to study free-base octaethylporphin (OEP) and α -chloro-octaethylporphin (α -Cl-OEP) in n-octane (n-C₈) and 2-methyl-tetrahydrofuran (MTHF) at 4.2 K. By selective laser excitation into the 0-0 transition a reversible photo-tautomerism was observed. Tautomer splittings between 10 and 100 cm⁻¹ were found. The vibrational frequencies of the ground state S₀ and the first excited singlet state S₁ were determined from fluorescence and excitation spectra and compared to other porphin molecules.

1. INTRODUCTION

It is known that optical spectra of unsubstituted porphin molecules incorporated in single n-alkane crystals at liquid helium temperature yield well resolved and simple spectra [1-4]. From ESR [2] and Zeeman experiments [3,5] it was established that the porphin molecules substitute a number of n-alkane chains, and are therefore oriented in well defined lattice sites. The spectra of rapidly cooled samples, however, become more complicated because thermodynamically less stable sites are formed [5,6]. In all cases the spectral bands are inhomogeneously broadened with widths of the order of a few cm^{-1} .

By means of photochemical hole-burning (PHB) [7,8] the spectral resolution can still be increased by a factor of 10^3 - 10^5 and the homogeneous linewidth can often be determined. Some free-base porphins, like H_2 -porphin (H_2P) [6,9-13] and H_2 -chlorin [14-16] have been studied by this method. The hole-burning mechanism in these molecules is a photo-tautomerism by which the two inner protons of the free-base porphin molecule are switched from one pair of opposite nitrogens to the other by selective laser excitation. In the case of H_2P (D_{2h} symmetry) no new chemical species is produced, and the phototautomerism takes place between two orientations of the H_2P molecule in a given lattice site. The difference in energy of these orientations is determined by the crystal field splitting, which is of the order of a few cm^{-1} to $\sim 100 \text{ cm}^{-1}$ [5,17]. In H_2 -chlorin, which differs from H_2P by the reduction of an outer bond in one of the pyrrole rings, the phototautomerism of the inner hydrogens leads to a molecule with a different chemical structure. Its absorption frequency lies $\sim 1500 \text{ cm}^{-1}$ above that of the original molecule [14].

Free-base octaethylporphin (OEP) (see fig. 1a), which is subject of our study is an H_2P -molecule with eight ethyl groups substituted on the outer pyrrole rings. Although its room temperature absorption spectrum is well known [19], and hole-burning experiments on OEP in polymer matrices at liquid helium temperature down to 0.05 K have been reported [19], no data seem to be available on the molecular vibrational frequencies. Furthermore, since OEP can

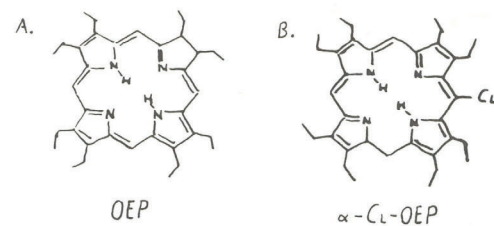


Fig. 1. Structure of the molecules that have been studied as guest in polycrystalline *n*-octane (*n*-C₈) and amorphous 2-methyl-tetrahydrofuran (MTHF) hosts.

- a. free-base octaethylporphyrin (OEP).
- b. free-base α -chloro-octaethylporphyrin (α -Cl-OEP).

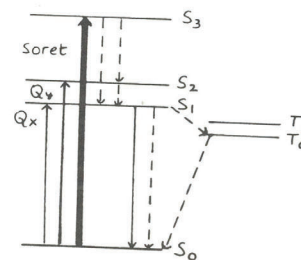


Fig. 2. Energy level diagram of the lower electronic states of free-base OEP. S and T represent singlet and triplet states respectively. The electronic transitions $S_1 + S_0$, $S_2 + S_0$ and $S_3 + S_0$ are called respectively the Q_x , Q_y and Soret bands.

be halogenated at the methine bridges [21-23], it gives the possibility to study nuclear quadrupole splittings in a porphyrin molecule by means of optical hole-burning in the MHz-regime. Such experiments are planned.

The energy level diagram of symmetric porphyrins, such as free-base OEP (see fig. 2) is characterized by a strong transition at about 400 nm, called the Soret band, and by two weaker transitions: the $S_1 + S_0$ (Q_x -band) and the $S_1 + S_0$ (Q_y -band). The lowest singlet state S_1 has a lifetime of the order of ns, whereas the lowest triplet state T_0 lives about ms. In free-base porphyrins the intersystem crossing (ISC) yield from S_1 to T_0 is ~ 90%, whereas only ~ 5% decays by fluorescence [23]. The decay from the triplet state is non-radiative.

The pathway for the photochemical hole-burning reaction in free-base porphyrin is believed to occur during ISC to the triplet state [9]. For H_2P the efficiency of the process was found to be ~ 1%, whereas for D_2P it was 1% [9], which shows that the inner protons play the key role in the hole-burning mechanism.

Here we report a study of OEP (fig. 1a) and α -Cl-OEP (fig. 1b) as guests in an n-octane crystalline host and in 2-methyl-tetrahydrofuran (MTHF) glassy host at 4.2 K. We have identified the principal sites of OEP and α -Cl-OEP in n-octane by photochemical hole-burning (PHB), and have recorded single-site fluorescence and absorption spectra of the $S_1 \leftrightarrow S_0$ transitions. We have also attempted to identify the $S_2 + S_0$ origin, as will be shown. From the results we could determine the internal molecular vibrations of OEP and α -Cl-OEP up to 1600 cm^{-1} . A qualitative comparison to vibrational frequencies of other free-base porphyrins is made in the last section.

2. EXPERIMENTAL

Free-base octaethylporphin (OEP), obtained from Aldrich Chem. Co., was used without further purification. Free-base α -chloro-octaethylporphin (α -Cl-OEP) was prepared in our laboratory [24] according to the method described in ref. [20]. 25 mg of OEP were dissolved in 40 ml of tetrahydrofuran, and refluxed for 30 minutes with a solution of H_2O_2 and HCl solution (resp. 0.3% and 36%). Subsequently, the mixture was diluted in 100 ml ether, washed thoroughly with water and $NaHCO_3$, and dried on $NaSO_4$ for 24 hs. The solution was chromatographed on an aluminium oxide column with hexane-toluene (1:1) as solvent. Three red bands could be distinguished. The slowest that came off, using dichloromethane as eluent, yielded α -Cl-OEP.

Both OEP and α -Cl-OEP were dissolved in n-octane ($n-C_8$) at low concentrations ($c = 4 \times 10^{-5}$ M to 4×10^{-7} M) and in 2-methyl-tetrahydrofuran (MTHF) at $c = 10^{-4}$ M. The concentrations were calculated from optical densities ($O.D. = \epsilon c d$) of various absorption bands at room temperature. The values of the extinction coefficients ϵ were taken from ref. [18]. The optical pathlength d was 1 mm. Polycrystalline samples of n-octane were obtained by quickly cooling the solution in liquid nitrogen before introducing it into the helium-bath cryostat.

Absorption spectra at room temperature were measured in a Shimadzu UV-360 spectrometer against air as reference. High resolution excitation and emission spectra at 4.2 K were measured with the experimental set-up shown in fig. 3. As excitation source we used the light of a pulsed dye laser (Molelectron DL-200, bandwidth $\sim 1 \text{ cm}^{-1}$) pumped by a nitrogen laser (Molelectron UV-22 laser, frequency 20 Hz), with the following dyes: PBB0 (391-411 nm), C495 (515-575 nm), R6G (570-605 nm), RB (595-630 nm) and DCM (630-670 nm). The emission (fluorescence) signal from the sample was either monitored with a 0.85 m double monochromator (Spex 1402, grating blazed at 1000 nm) used in second order (bandwidth $\sim 3\text{-}12 \text{ cm}^{-1}$) or detected broad band by a cooled photomultiplier (EMI 9659 B). A Schott R 665 cut-off filter was placed in front of the photomultiplier to separate the fluorescence from the excitation light. The signal of the photomultiplier was amplified by a Keitley 610 C

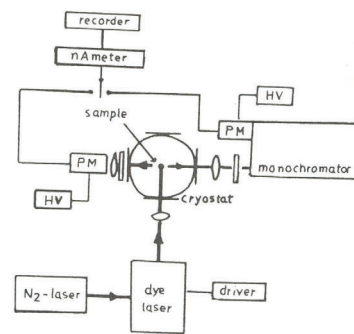


Fig. 3. Experimental set-up for spectroscopic studies at low temperature (1.2 - 4.2 K). The apparatus at the right of the cryostat is used for high resolution detection, that at the left for broad band detection. PM: photomultiplier. HV: high voltage generator.

electrometer.

Fluorescence spectra with broad band excitation were obtained by irradiating the Soret-band at 400 nm, whereas single-site fluorescence spectra were obtained by exciting the 0-0 band or a vibration of the $S_1 \leftarrow S_0$ transition of a specific site, and scanning the monochromator through the emission spectrum. In the case of broad band excitation we used a RG 435 cut-off filter to avoid excitation light in third order to be detected by the monochromator.

Absorption spectra at 4.2 K were taken in the form of fluorescence excitation spectra: the pulsed dye laser was scanned through the absorption spectrum, and the fluorescence signal was detected either broad band by monitoring it with $\lambda \geq 665$ nm (0-0 band excluded), or by site-selection of the emission using a fixed wavelength set by the monochromator (the 0-0 band or a vibrational band of the $S_1 \rightarrow S_0$ transition of a specific site). In order to obtain the molecular vibrations with a good signal-to-noise ratio, single site excitation spectra were obtained by burning away the complementary 0-0 line of a specific site.

The wavelength reading of the pulsed dye laser was calibrated against that of the 0.85 m monochromator, whereas the latter was calibrated by means of Hg- and Ne-lamps (Oriel). Neither correction for the wavelength dependence of the monochromator response nor for the photomultiplier sensitivity were applied. The spectral intensities were roughly corrected for the wavelength dependence of the dye-output.

3. RESULTS AND DISCUSSION

3.1. OCTAETHYLPORPHIN

The absorption spectrum of free-base octaethylporphyrin (OEP) in n-octane at room temperature is given in fig. 4. It shows four weak bands of O.D. = 0.02 between 630 and 470 nm: the origin of the $S_1 + S_0$ transition (Q_x -band) at ~ 623 nm and its vibrational region at ~ 567 nm, and two bands at ~ 526 and 495 nm, that we attribute to the $S_2 + S_0$ transition (Q_y -region). The very strong peak (O.D. = 0.25) at 396 nm is the Soret-band. The width of these bands are of the order of a few hundred cm^{-1} .

Fig. 5a shows a broad band detected excitation spectrum of the 0-0 transition region of OEP in n-C₈ at 4.2 K. Notice that by lowering the temperature the optical resolution has increased to a few wavenumbers. Various sites between 615 and 623 nm are observed in the spectrum, the three most prominent of which have been called K, L and M in order of reducing energy (see table 1). They have been identified by means of hole-burning. This was done by irradiating, for example, the M_2 -band (see fig. 5b) with the laser at 623.0 nm, and observing that its intensity decreases (or burns away), while another spectral band at 622.2 nm (M_1) grows in. This process is reversible: by burning away the M_1 -band (fig. 5c), the M_2 -band increases. This behaviour was observed for all sites and is similar to that of free-base porphyrin (H_2P) [6,9-13,16], where the double spectrum corresponds to two orientations of the molecule in a given lattice site. By burning into one of these orientations the two inner hydrogens are transformed from one pair of opposite nitrogens to the other, which is equivalent to a $\pi/2$ rotation of the entire molecule in the host lattice. The spectral distance (crystal field splitting) between the two M-lines is 21 cm^{-1} .

The 0-0 transition frequencies and the corresponding crystal field splittings for the different sites are listed in table 1. The crystal field splittings are of the same order as for free-base porphyrin in n-alkane crystals [5,17].

At 4.2 K not only the 0-0 region becomes highly resolved, but also the

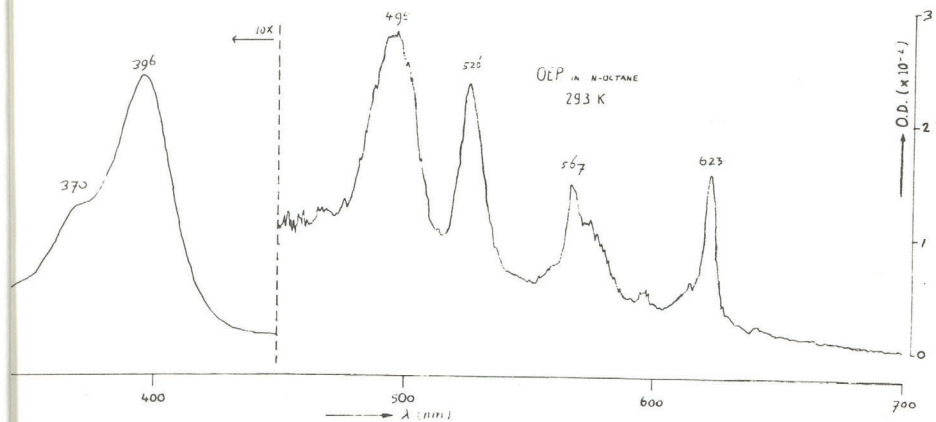


Fig. 4. Room temperature absorption spectrum of OEP in n-octane crystal. The absorption bands at 623 and 567 nm belong to the $S_1 + S_0$ (Q_x) transition, those bands at 526 and 495 nm to the $S_2 + S_0$ (Q_y) transition. The strong Soret band at ~ 400 nm corresponds to the $S_3 + S_0$ electronic transition.

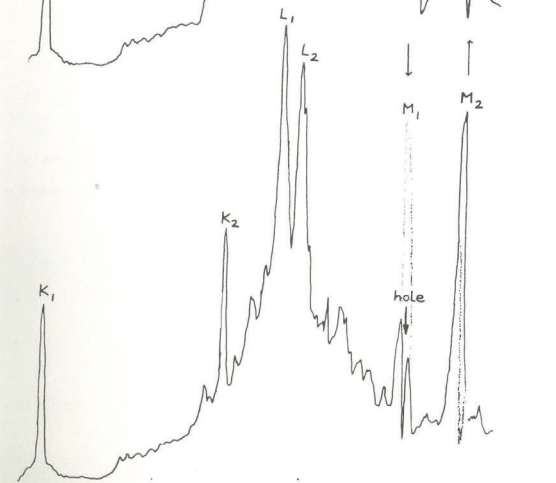
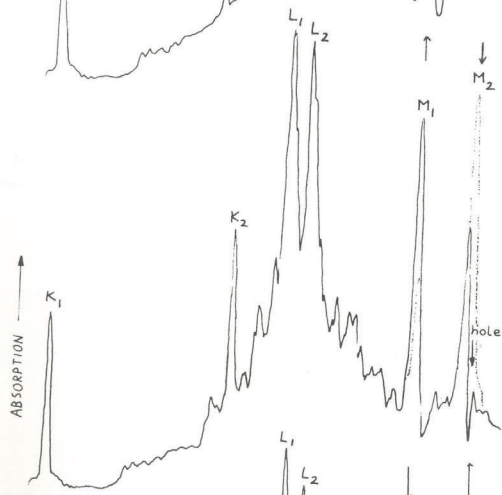
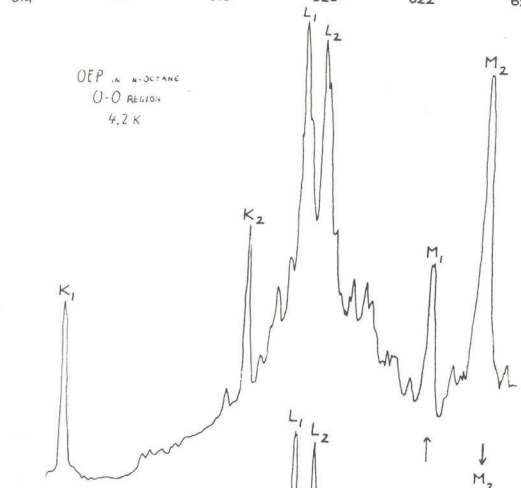
(NEXT PAGE)

- Fig. 5. Broad band detected fluorescence excitation spectra of the $S_1 + S_0$ transition of OEP in n-octane crystal at 4.2 K.
- The 0-0 region shows various sites, the largest of which we called K, L and M.
 - The same region after 1 min. irradiation with a laser at the M_2 0-0 band. The molecules absorbing at this wavelength phototransform into M_1 . A hole is burnt into the M_2 -band.
 - The same region after 1 min. irradiation into site M_1 . Notice the hole burnt into this band. A similar reversible photochemical hole-burning process was observed for sites L and M.

→ λ (nm)

614 616 618 620 622 624

OEP IN N-HEPTANE
O-O REGION
4.2 K



16200 16100 16000

Table 1. Spectral positions of the $S_1 + S_0$ 0-0 lines of the K, L and M sites of OEP in n-octane, and their corresponding tautomer splittings.

Site	Position of the 0-0 band		Tautomer splitting $\Delta\tilde{\nu}$ (cm^{-1})
	λ (nm)	$\tilde{\nu}$ (cm^{-1})	
K ₁	615,08	16258	96
K ₂	618,72	16162	
L ₁	619,78	16135	10
L ₂	620,15	16125	
M ₁	622,38	16067	21
M ₂	623,19	16046	

individual vibrations of the $S_1 \leftarrow S_0$ transition. This is shown in fig. 6a, where a broad band detected excitation spectrum is shown up to $\sim 700 \text{ cm}^{-1}$ above the origin. An excitation spectrum site-selected in the 0-0 transition of L_1 is shown in fig. 6b as comparison. In this spectrum only vibrations of the $S_1 \leftarrow S_0$ transition of the L_1 -site are visible. Notice that the characteristic pattern of close lying doublets in the broad band detected spectrum corresponds to vibrations of the L-site. Site-selected excitation spectra have also been obtained for the other sites, from which the vibrational frequencies up to 1600 cm^{-1} above 0-0 could be determined. The vibrational frequencies of the S_1 -state for five different sites of OEP in n-octane are listed in table 2. We have included in the table the S_1 - and S_0 -state vibrational frequencies of OEP in 2-methyl-tetrahydrofuran (MTHF), for comparison. The latter have been obtained from site-selected (in the 0-0 transition) excitation and fluorescence spectra respectively. Notice that the vibrational frequencies in the different sites and in the two hosts do not differ, in general, by more than 10 cm^{-1} . The similarities between the vibrational frequencies in the ground S_0 and first excited singlet state S_1 suggest that OEP changes its shape only slightly by excitation into S_1 .

It should be remarked that MTHF forms a glass at low temperature and, due to its disordered structure, it yields much larger inhomogeneous spectral linewidths (a few 100 cm^{-1} broad) than crystalline n-alkanes (a few cm^{-1} broad). An example of a broad band detected excitation spectrum of OEP in MTHF at 4.2 K is shown in fig. 7. Notice that a hole has been burnt in the 0-0 region at $\sim 618.2 \text{ nm}$.

By selecting the fluorescence wavelength (fig. 8) or the excitation wavelength (fig. 9) the spectral bands are narrowed by a factor of ~ 100 (!), and the vibrational frequencies can be determined as accurately as in the case of OEP in crystalline n-octane. In fig. 8 the vibrations of the S_1 -state of OEP in MTHF between 700 and 1250 cm^{-1} above the origin are given, whereas the vibrations of the S_0 -state between 100 and 1600 cm^{-1} below the origin are shown in fig. 9.

Much more difficult to determine accurately is the origin of the $S_2 \leftarrow S_0$ transition, also called the Q_y -band. Two criteria have been used by

Fig. 6. Fluorescence excitation spectra of OEP in n-octane crystal at 4.2 K.

- a. Broad band detected at $\lambda > 665$ nm. Notice the 0-0 (between ~ 615 - 630 nm) and the vibrational bands ($\lambda \leq 612$ nm) of different sites. The vibronic frequencies of the L-site with respect to the origin are given in cm^{-1} .
- b. Site selected detection at the 0-0 band of L_1 (16135 cm^{-1}). The positions of the vibronic bands relative to their origin are given in cm^{-1} .

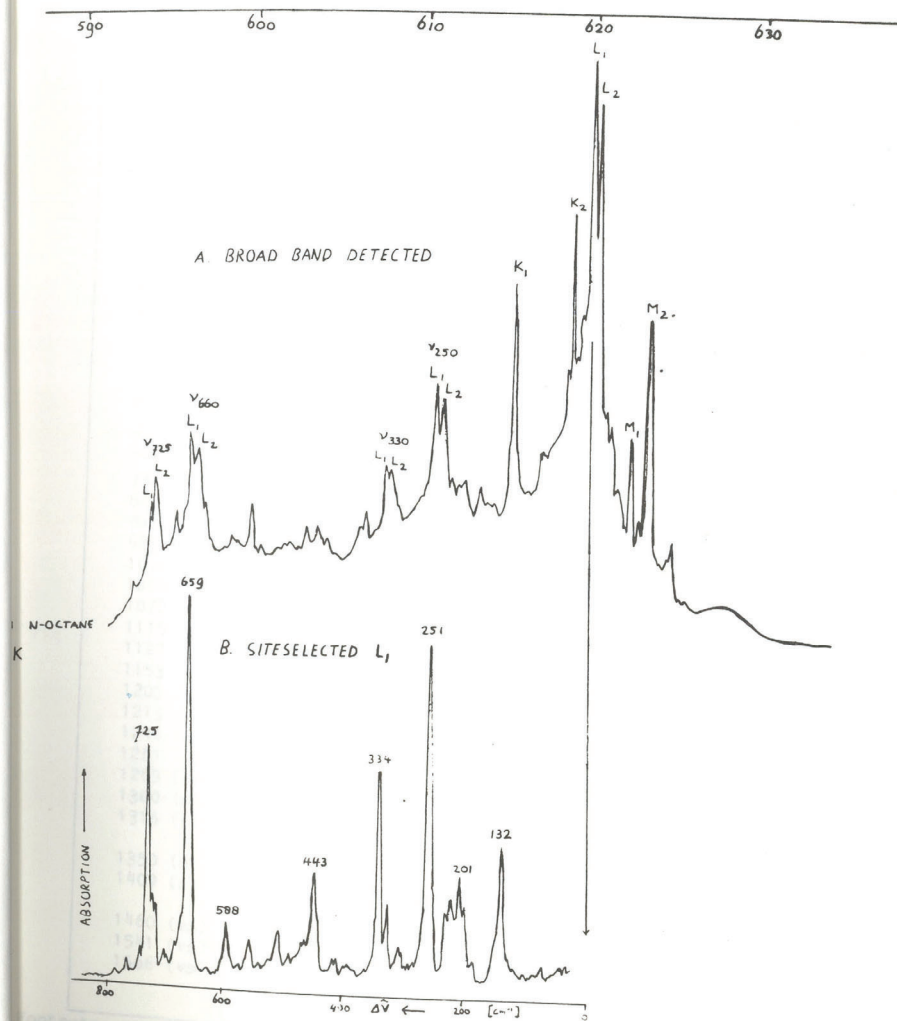


Table 2. The first excited singlet S_1 -state vibrational frequencies ν_1 (cm^{-1}) of five sites of OEP in n-octane, and the ground S_0 - and excited S_1 -state vibrational frequencies ν_1 (cm^{-1}) of OEP in MTHF.

n-octane					MTHF	
K_1	K_2	S_1		M_2	S_1	S_0
		L_1	L_2			
138 (mw)	139 (ms) 184 (vw)	132 (m) 176 (vw) 194 (mw)	137 (s) 177 (mw) 188 (mw)	132 (mw) 181 (mw) 190 (mw)	134 (m) 177 (w)	129 (m) 171 (m)
204 (m)	197 (ms) 216 (w)	201 (m) 214 (mw) 222 (mw)	220 (m)	199 (w) 221 (w) 232 (w)	204 (m) 212 (m)	202 (m)
246 (m)	244 (m)			252 (m)		
251 (m)	251 (s)	251 (s)	253 (s)	252 (m)	258 (m)	251 (s)
263 (w)	262 (m)			270 (w)	272 (vw)	
287 (w)	282 (w)		281 (w)			
298 (w)	288 (w) 319 (m)	298 (w) 319 (m)	296 (w) 323 (w)			
338 (ms)	334 (vs)	334 (s)	336 (s)	331 (m)	338 (m)	333 (m)
419 (w)			413 (w)			
449 (mw)	448 (w) 483 (mw)	441 (m) 499 (mw)	437 (w) 487 (w)	438 (mw) 495 (w)	459 (w)	
510 (w)	508 (m)		502 (w)	507 (w)	511 (w)	
523 (w)	526 (w)	519 (w)	519 (w)	523 (w)	523 (w)	
539 (w)			541 (w)	535 (w)	536 (w)	
553 (w)	549 (w)	549 (w)		549 (w)		
591 (mw)	590 (m)	588 (m)	589 (mw)	592 (mw)	586 (w)	
657 (vs)	655 (vs)	659 (vs)	653 (vs)	647 (s)	649 (vs)	649 (s)
712 (m)	712 (vw)	712 (w)	710 (vw)	710 (vw)		
726 (vs)	725 (vs)	725 (vs)	727 (vs)	725 (s)	722 (vs)	727 (s)
759 (w)			760 (w)	762 (w)	755 (w)	758 (s)
784 (w)			777 (w)	776 (w)	781 (w)	
892 (w)				889 (mw)	889 (mw)	
948 (mw)				946 (m)	945 (m)	942 (m)
980 (w)				981 (w)	975 (w)	
1014 (s)				1013 (m)	1011 (s)	1011 (m)
1059 (m)				1064 (mw)	1059 (mw)	
1078 (s)				1080 (s)	1079 (s)	
1115 (s)				1111 (m)	1114 (s)	
1127 (m)				1125 (mw)	1128 (mw)	1125 (ms)
1153 (mw)				1147 (m)	1147 (mw)	
1203 (s)				1198 (vs)	1201 (vs)	1210 (s)
1213 (s)				1212 (s)		
1246 (m)				1237 (s)		
1261 (mw)				1260 (mw)		
1269 (s)				1275 (m)		
1300 (m)				1312 (s)		
1316 (s)				1321 (vs)	1323 (s)	
				1335 (w)		
1350 (s)			1347 (m)	1347 (s)		
1409 (s)			1406 (s)	1408 (s)		
						1420 (m)
1460 (ms)			1461 (ms)	1450 (m)		
1541 (vs)			1537 (vs)		1533 (vs)	1543 (s)
1566 (vs)			1558 (vs)		1551 (vs)	
						1583 (vs)
						1609 (s)

Footnote: the intensities of the spectral bands are indicated in parenthesis s (strong), m (medium), w (weak) and v (very).

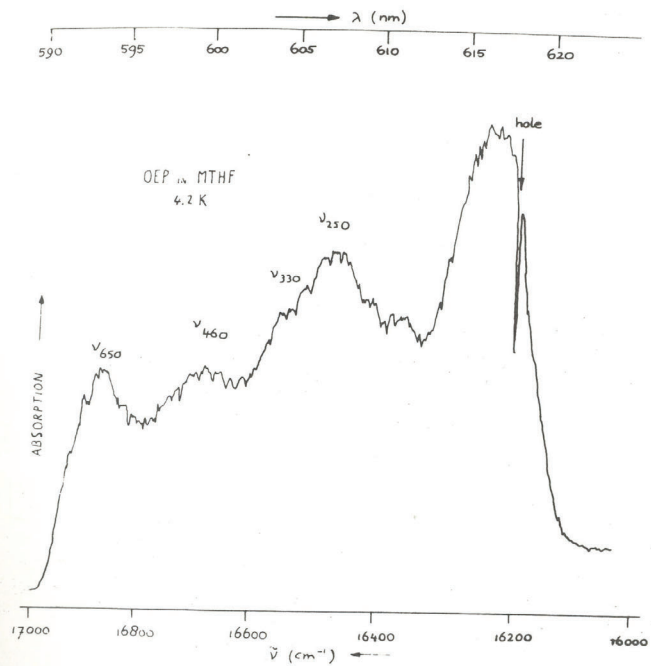


Fig. 7. Broad band detected fluorescence excitation spectrum of OEP in MTHF glass at 4.2 K. A hole has been burnt into the red wing of the 0-0 absorption band. Its width is limited by the bandwidth of the laser of $\sim 1 \text{ cm}^{-1}$. Broad vibrational bands of the $S_1 \leftarrow S_0$ transition are indicated in cm^{-1} (from 0-0).

Fig. 8. High resolution
at 4.2 K
of the
origin

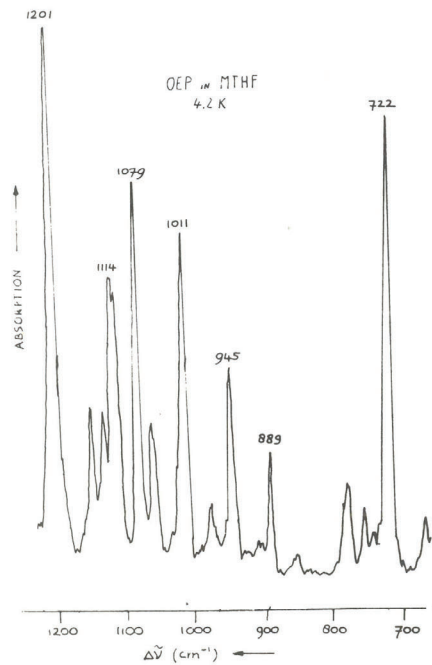


Fig. 8. High resolution fluorescence excitation spectrum of OEP in MTHF glass at 4.2 K site-selected at 16219 cm^{-1} (0-0 band) at 4.2 K. Positions of the $S_1 \leftarrow S_0$ vibronic peaks are given in cm^{-1} relative to the origin.

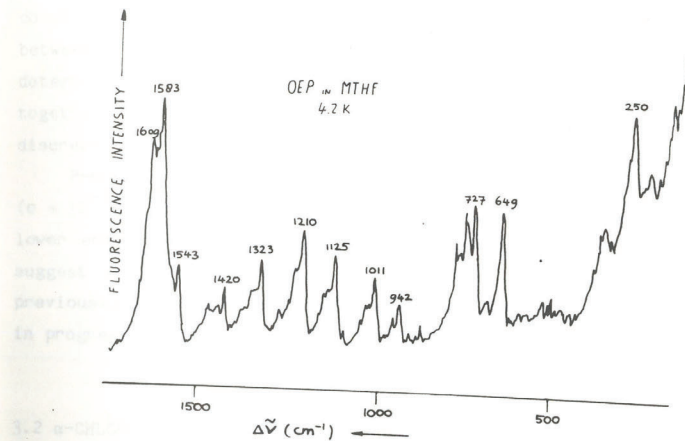


Fig. 9. Fluorescence spectrum of OEP in MTHF glass site-selectively excited at 16189 cm^{-1} (0-0 band) at 4.2 K. Positions of the $S_1 + S_0$ vibrations are given in cm^{-1} relative to the origin.

us. None of them, however, yield a satisfactory result. If we take the first absorption band which is stronger than some weak features that still seem to belong to the $S_1 + S_0$ transition, we would choose a band at 540.2 nm, which is at 2254 cm^{-1} from the Q_x -origin (K_1 -site). With the second criterion, namely taking the first band for which the vibrational frequencies have approximately the same values as those of the Q_x -band, we would choose a band at 536.1 nm, which is at 2395 cm^{-1} from the origin of the Q_x -band (K_1 -site). Thus, we conclude from these results that the Q_x - Q_y distance for the K_1 -site lies between ~ 2250 and 2400 cm^{-1} , which is about 700 cm^{-1} smaller than the value determined for H_2P [11,25]. More accurate measurements in various hosts together with polarization experiments are necessary to solve this discrepancy.

Preliminary experiments on OEP in MTHF at high concentrations ($c \approx 10^{-3} \text{ M}$) show the formation of a dimer or aggregate band at 600 cm^{-1} to lower energy of the 0-0 transition. Single-site excitation spectra at 4.2 K suggest that a splitting of a few cm^{-1} occurs in various vibrational bands as previously observed in H_2P [26]. Current studies of this surprising effect are in progress.

3.2 α -CHLORO-OCTAETHYLPORPHIN

Similar experiments as on octaethylporphin (OEP) were performed on free-base α -chloro-octaethylporphin (α -Cl-OEP). An example of a broad band detected absorption spectrum of α -Cl-OEP in $n\text{-C}_8$ at 4.2 K is shown in fig. 10a. Notice that the 0-0 region between ~ 622 and 628 nm is shifted $\sim 100\text{-}200 \text{ cm}^{-1}$ to lower energy with respect to that of OEP.

Four principal sites, called N, O, P and Q have been studied. As in the case of OEP, all sites appear double and they can be reversibly burnt into each other. Table 3 gives the spectral positions of the 0-0 lines for each site. We should remark here that there is a partial overlap between the O_2 and the P_2 bands, which we were able to unravel by hole-burning. Irradiating the red wing of the band at 626.82 nm (P_2), its corresponding P_1 -site at 626.09 nm

Table 3. Spectral positions of the $S_1 \leftarrow S_0$ 0-0 lines of the N, O, P and Q sites of α -Cl-OEP in n-octane, and their corresponding tautomer splittings.

Site	Position of the 0-0 band		Tautomer splitting $\Delta\tilde{\nu}$ (cm^{-1})
	λ (nm)	$\tilde{\nu}$ (cm^{-1})	
N ₁	622.14	16074	67
N ₂	624.75	16006	
O ₁	623.09	16049	93
O ₂	626.73	15956	
P ₁	626.09	15972	19
P ₂	626.82	15954	
Q ₁	627.10	15947	19
Q ₂	627.84	15928	

increases, and vice versa. By burning, however, in the blue wing (O_2) a band at 623.13 nm (O_1) grows in. This process is reversible. The fact that the band at ~ 626.8 nm is an overlap of two sites can further be concluded from a broad band excited fluorescence spectrum (fig. 11), where this band shows a clear splitting.

It should be noticed that the absorption bands around 620 nm in fig. 10a belong to 0-0 transitions of OEP, which is still present as impurity in our sample of α -Cl-OEP. In addition, we found an overlap between the N_1 - and O_1 -bands of α -Cl-OEP with, respectively, the M_1 and M_2 bands of OEP. Nevertheless, spectra of pure α -Cl-OEP were obtained by site-selection, either in excitation or emission.

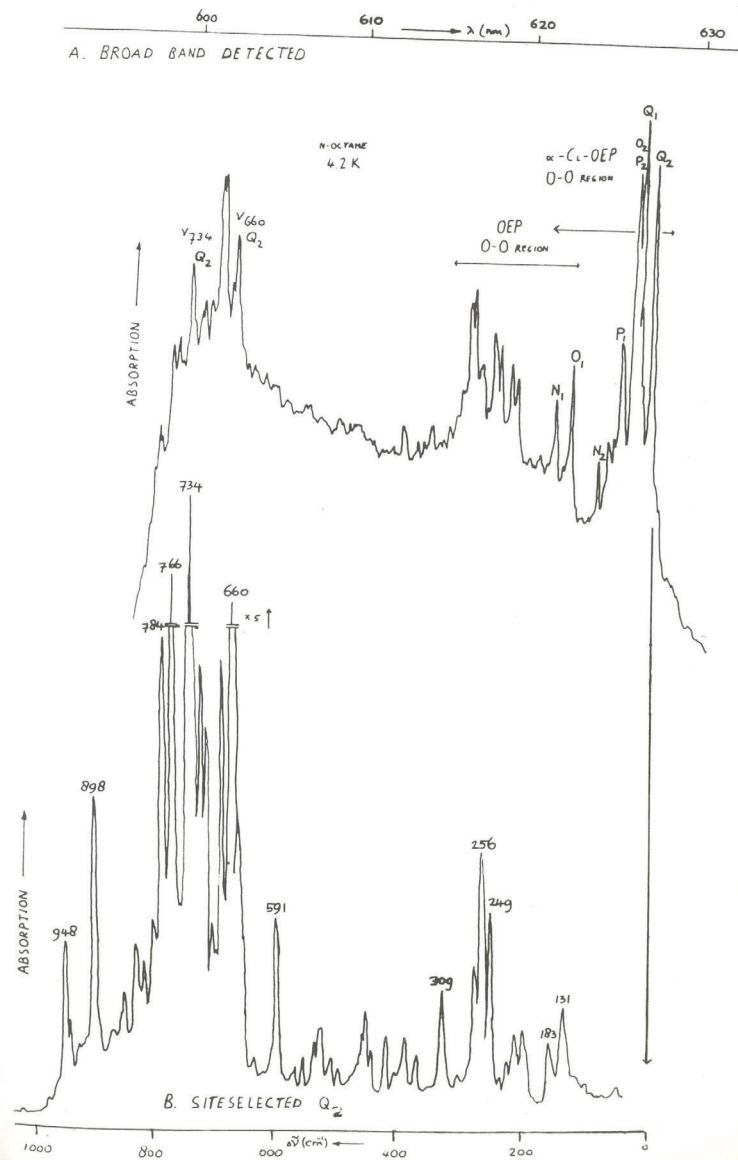
In order to determine the molecular vibrational frequencies of the $S_1 + S_0$ transition of α -Cl-OEP, site selected excitation spectra were taken like that shown in fig. 10b. In this spectrum vibrations of the Q_2 -site between the origin and up to 950 cm^{-1} above the origin are observed. A list of the vibrational frequencies of the $S_1 + S_0$ transition for four different sites, N_2 , O_2 , Q_1 and Q_2 , is given in table 4, together with the vibrational frequencies of the $S_1 + S_0$ transition for site Q_2 . The latter were determined by means of a fluorescence spectrum excited with the laser in the 724 cm^{-1} vibrational band of this site. As found for OEP, the frequencies in the first excited singlet state S_1 are very similar to those in the ground state S_0 , which suggests that OEP and α -Cl-OEP do not change their shape significantly by excitation into the S_1 .

3.3. COMPARISON OF OEP, α -Cl-OEP AND VARIOUS FREE-BASE PORPHINS

In table 5 the vibrational frequencies of OEP, α -Cl-OEP, H_2P [17], tetra-deuterated H_2P (H_2P-d_4) [27] and tetraphenylporphin (TPP) [28] (all free-base) are given. The frequencies of OEP and α -Cl-OEP, in columns 1 and 2 respectively, are rather similar to each other with the exception of a few vibrations. For example, the strong vibrations at 1079 (s) and 1272 (ms) cm^{-1} are present in OEP but absent in α -Cl-OEP, whereas those at 690 (s), 823 (m),

Fig. 10. Fluorescence excitation spectra of α -Cl-OEP in n-octane crystal at 4.2 K.

- Broad band detected at $\lambda \geq 665$ nm. Notice the 0-0 and vibrational bands of various sites of α -Cl-OEP. OEP is present as an impurity. Vibronic frequencies of site Q_2 are given in cm^{-1} with respect to the origin.
- Site selected detection at 15930 cm^{-1} (Q_2 0-0 band). Positions of the vibronic $S_1 \leftarrow S_0$ peaks are given in cm^{-1} relative to the origin.



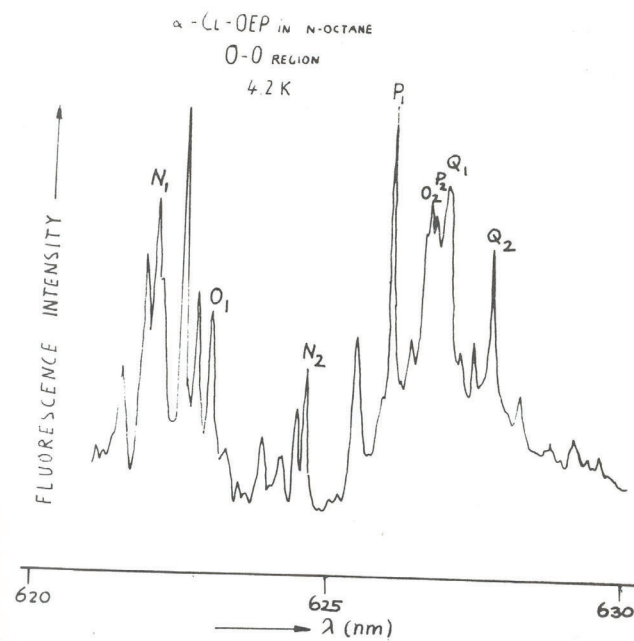


Fig. 11. Fluorescence spectrum of the $S_1 + S_0$ 0-0 transition of α -Cl-OEP in n-octane crystal at 4.2 K excited into the Soret band at 400 nm. The largest sites have been called N, O, P and Q. Other intense lines belong to $S_1 + S_0$ vibrations of the OEP impurity.

Table 4. The first excited singlet S_1 -state vibrational frequencies ν_i (cm^{-1}) of four sites of α -Cl-OEP in n-octane, and the ground S_0 -state vibrational frequencies ν_i (cm^{-1}) of site Q_2 of α -Cl-OEP in n-octane.

N_2	S_1			S_0
	Q_2	Q_1	Q_2	Q_2
				34 (s) 75 (s)
130 (m) 181 (w)	133 (m)	130 (m w)	112 (w) 131 (m w)	136 (m)
194 (m) 218 (m w)	197 (m) 208 (m w)	194 (m w) 215 (w)	183 (m w) 218 (w)	184 (m)
246 (m) 252 (m) 264 (w) 286 (w)	245 (m) 253 (m) 266 (w) 288 (w)	245 (m) 258 (m) 268 (m w)	245 (m) 255 (m) 273 (m) 292 (w)	240 (m) 260 (m) 276 (m)
303 (w) 326 (m)	306 (w) 327 (m w)	299 (w) 323 (m w)	309 (m w) 320 (w)	332 (w)
417 (w) 439 (w)	371 (m w) 437 (m w)	381 (m w) 413 (m w)	379 (m w) 409 (w)	404 (s)
487 (m w) 510 (w)	464 (m w) 492 (m w) 501 (w)	451 (m w) 490 (w) 501 (w)	461 (w) 490 (m w)	
517 (w) 529 (w) 540 (m w)	518 (m w) 528 (w)	518 (m w) 529 (w)	517 (m w) 528 (w)	
555 (w) 594 (m) 661 (vs)	553 (m w) 597 (m w) 656 (vs)	561 (w) 590 (m) 663 (vs)	555 (w) 591 (m) 660 (vs)	
688 (m) 713 (m) 734 (vs)	692 (s) 712 (s) 734 (vs)	682 (s) 711 (s) 734 (vs)	709 (s) 732 (vs)	711 (w) 749 (w)
768 (s) 779 (s)	767 (s) 782 (s)	766 (vs) 784 (s)	764 (vs) 776 (s)	780 (w)
		809 (w)	805 (w)	800 (w)
	826 (m) 844 (m)		820 (m w) 843 (m w)	
893 (s)	896 (s)	898 (s)	894 (s)	
947 (s) 1016 (s)	947 (s)	948 (s)	949 (m w) 1009 (s) 1020 (m w)	929 (w) 955 (w) 1000 (m)
1098 (s) 1121 (m) 1153 (w) 1167 (w) 1202 (vs)			1114 (s) 1124 (m) 1149 (m) 1165 (w)	1022 (m) 1113 (m)
		1198 (s)	1205 (m)	1147 (w) 1164 (w)
1235 (m) 1253 (w)			1224 (m) 1254 (m)	1219 (m)

Table 4. (Cont.)

N ₂	S ₁			S ₀
	O ₂	Q ₁	Q ₂	Q ₂
1263 (w)				
1277 (m)				
1306 (m)			1300 (m)	
1314 (m)				
1320 (s)			1317 (m)	
1344 (s)			1341 (s)	1351 (s)
1363 (m)			1359 (m)	
1407 (s)			1403 (s)	1402 (w)
1417 (s)			1411 (s)	1427 (m w)
1447 (m)			1446 (m)	
1487 (s)			1481 (s)	1499 (w)
1544 (vs)		1537 (s)	1527 (s)	
1568 (vs)		1563 (s)	1556 (s)	
1592 (m)			1585 (m)	1576 (s)
1604 (w)			1596 (w)	1590 (s)
			1614 (m w)	1606 (s)
1631 (w)				

Footnote: the intensities of the spectral bands are indicated in parenthesis s (strong), m (medium), w (weak) and v (very).

Table 5. Vibrational frequencies ν_i (cm^{-1}) of the first excited singlet S_1 -state of octaethylporphyrin (present work), alpha-chloro-octethylporphyrin (present work), free-base porphyrin [17], tetra-deuterated free-base porphyrin [27] and tetraphenylporphyrin [28].

OEP a)	α -Cl-OEP a)	H_2P a)	$\text{H}_2\text{P-d}_4$ a)	TPP b)
134 (m)	132 (m)		118 (m)	
180 (m w)	190 (m w)	155 (s)	155 (w)	166 (w)
201 (m)	215 (m w)			
249 (m)	244 (m)			203 (m)
252 (m)	256 (m)			247 (w)
265 (w)	270 (m w)			
	288 (w)			
298 (w)	303 (m w)			
320 (m)				
334 (s)				
	326 (m w)			319 (m)
	380 (m w)	308 (s)	308 (m)	337 (vs)
	410 (m w)			
445 (m w)	439 (m w)			
	460 (m w)			
490 (m w)	490 (m w)			
510 (w)	505 (w)			
	518 (m w)			
523 (w)	528 (w)			
540 (w)	545 (w)			
550 (w)	555 (m w)			
589 (m w)	593 (m)		611 (w)	
653 (vs)	661 (vs)		657 (s)	
	690 (s)			
712 (w)	712 (s)			
725 (vs)	737 (vs)	710 (s)		
				738 (w)
759 (w)	766 (s)			748 (w)
780 (w)	780 (s)		762 (m)	
	805 (w)	783 (m)		
	823 (m)			
890 (m w)	895 (s)			820 (m)
			909 (m)	
945 (m)			923 (m)	
979 (w)	949 (s)	943 (s)	951 (s)	954 (vs)
		970 (w)		970 (m)
		987 (m w)		
		993 (m w)	998 (w)	
1012 (ms)	1008 (s)	1018 (w)	1018 (m)	
	1020 (m w)			
1060 (m w)				
1079 (s)				
1113 (s)		1052 (m)		1065 (w)
1126 (m w)	1108 (s)	1109 (m)	1070 (m w)	1119 (m)
1149 (m w)	1123 (m)			
	1150 (m w)			
			1142 (m)	

Table 5. (Cont.)

OEP ^{a)}	α -Cl-OEP ^{a)}	H ₂ P ^{a)}	H ₂ P-d ₄ ^{a)}	TPP ^{b)}
	1165 (mw)	1161 (m)	1180 (w)	1192 (m)
1203 (vs)	1202 (s)	1210 (s)	1199 (m)	1204 (s)
1212 (s)	1220 (ms)			1219 (w)
1242 (ms)	1254 (mw)		1256 (ms)	1258 (w)
1260 (mw)				
1272 (ms)			1269 (ms)	
1306 (ms)	1303 (m)	1297 (s)		1305 (w)
1320 (s)	1319 (ms)			1315 (m)
1335 (w)		1340 (m)		
1348 (s)	1345 (s)	1355 (s)	1354 (m)	1354 (vs)
	1360 (m)			
	1404 (s)			
1410 (s)	1418 (s)			1424 (m)
				1433 (w)
1457 (ms)	1447 (m)			1462 (s)
	1489 (s)	1478 (m)	1487 (w)	
				1504 (vs)
1539 (vs)	1536 (vs)	1552 (s)		1541 (m)
1560 (vs)	1562 (vs)	1588 (s)		1558 (w)
	1584 (s)			
1609 (s)?	1600 (s)?			

a) solvent n-octane.

b) solvent nitrobenzene.

Footnote: the intensities of the spectral bands are indicated in parenthesis
s (strong), m (medium), w (weak) and v (very).

1360 (m), 1404 (s) and 1484 (s) cm^{-1} are present in $\alpha\text{-Cl-OEP}$ and not in OEP. It is most probable that the latter are specifically related to the chlorine substitution in one of the methine bridges of $\alpha\text{-Cl-OEP}$.

If we compare the vibrations of H_2P [17] with those of OEP and $\alpha\text{-Cl-OEP}$, we notice that there are many more vibrations present in the latter two. This can be understood in terms of the eight ethyl-groups substituted at the pyrrole rings of OEP. There are also a few vibrations present in H_2P and absent in OEP and $\alpha\text{-Cl-OEP}$: 118 (m), 155(s), 308 (s), 970 (m) and 1478 (m). It may be that these vibrations appear shifted in frequency in OEP, due to the larger structure of this molecule. We tentatively assign the following correspondence between vibrations of H_2P and OEP: 155 (s) \rightarrow 134 (m), 308 (s) \rightarrow 334 (s), 1478(m) \rightarrow 1489 (s).

By comparing the vibrational frequencies of $\text{H}_2\text{P-d}_4$ [27] with those of H_2P one is tempted to associate them with the deuteration at the four methine bridges. However, many of the frequencies that appear in $\text{H}_2\text{P-d}_4$ are also present in OEP and $\alpha\text{-Cl-OEP}$. Thus, it is difficult to make assignments without additional information.

In column 5 we have listed vibrational frequencies of TPP in nitrobenzene taken from the literature [28], since there are no data available, to our knowledge, on TPP in n-alkane crystals. As for the case of $\text{H}_2\text{P-d}_4$, it is difficult to establish an unambiguous correspondence to vibrations related to the methine groups. One can only say with certainty that the larger structures of the TPP- and the OEP-molecules are responsible for the extra-vibrations, when we compare them to those of H_2P .

4. CONCLUSIONS

We have shown that highly resolved optical spectra with a resolution of a few cm^{-1} can be obtained in OEP and $\alpha\text{-Cl-OEP}$, two substituted free-base porphyrin molecules, incorporated in both crystalline n-alkane matrices and

organic glasses at 4.2 K. From single-site fluorescence and excitation spectra we were able to identify the internal molecular vibrations of the ground S_0 and first excited singlet state S_1 of both molecules up to 1600 cm^{-1} . We have further shown that a phototautomerism occurs at liquid helium temperature, as previously found for H_2P . The two tautomers are reversibly interconverted by selective laser excitation. Their crystal field splitting is of the order of 10 to 100 cm^{-1} , depending on the site. In addition, we have identified new spectral bands at $\sim 600\text{ cm}^{-1}$ to the red from the 0-0 bands, which we attribute to dimer molecules of OEP.

ACKNOWLEDGEMENTS

The investigations were supported by the Netherlands Foundation for Physical Research (F.O.M.) with financial aid from the Netherlands Organisation for the Advancement of Pure Research (Z.W.O.).

REFERENCES

- [1] I.Y.Chan, W.G. van Dorp, T.J. Schaafsma and J.H. van der Waals, Mol. Phys. 22 (1971) 741,753.
- [2] W.G. van Dorp, M. Soma, J.A. Kooter and J.H. van der Waals, Mol. Phys. 28 (1974) 1551; W.G. van Dorp, W.H. Schoemaker, M. Soma and J.H. van der Waals, Mol. Phys. 30 (1975) 1701.
- [3] G. Jansen, M. Noort, N. van Dijk and J.H. van der Waals, Mol. Phys. 39 (1980) 865.

- [4] G.W. Canters and J.H. van der Waals, in *The Porphyrins*, Vol. III, ed. D. Dolphin (Academic Press, New York, 1978) p. 53 and references therein.
- [5] G. Jansen, thesis, University of Leyden (1977).
- [6] S. Völker, R.M. Macfarlane, A.Z. Genack, H.P. Trommsdorff and J.H. van der Waals, *J. Chem. Phys.* 67 (1977) 1759.
- [7] A.A. Gorokhovskii, R.K. Kaarli and L.A. Rebane, *J. Exp. Theor. Phys. Lett.* 20 (1974) 216.; *Opt. Comm.* 16 (1976) 91.
- [8] B.M. Kharlamov, R.I. Personov and L.A. Bykovskaya, *Opt. Comm.* 12 (1974) 191.
- [9] S. Völker and J.H. van der Waals, *Mol. Phys.* 32 (1976) 1703.
- [10] S. Völker, R.M. Macfarlane and J.H. van der Waals, *Chem. Phys. Lett.* 53 (1978) 8.
- [11] A.I.M. Dicker, M. Noort, S. Völker and J.H. van der Waals, *Chem. Phys. Lett.* 73 (1980) 1.
- [12] A.I.M. Dicker, thesis, University of Leyden (1982).
- [13] H.P.H. Thijssen, thesis, University of Leyden (1985).
- [14] S. Völker and R.M. Macfarlane, *J. Chem. Phys.* 73 (1980) 4476.
- [15] A.I.M. Dicker, M. Noort, H.P.H. Thijssen, S. Völker and J.H. van der Waals, *Chem. Phys. Lett.* 78 (1981) 212.
- [16] A.I.M. Dicker, J. Dobkowski, M. Noort, S. Völker and J.H. van der Waals, *Chem. Phys. Lett.* 88 (1982) 135.
- [17] R.M. Macfarlane and S. Völker, *Chem. Phys. Lett.* 69 (1980) 151.
- [18] M. Gouterman, in *The Porphyrins*, Vol. III, ed. D. Dolphin (Academic Press, New York, 1978) p. 16 and references therein.
- [19] A.A. Gorokhovskii, V. Korrovits, V. Palm and M. Trummal, *Chem. Phys. Lett.* 125 (1986) 355.

- [20] R. Bonnett, I.A.D. Gale and G.F. Stephenson, J. Chem. Soc. (C) (1966) 1600.
- [21] E. Samuels, R. Shuttleworth and T.S. Stevens, J. Chem. Soc. (C) (1968) 145.
- [22] J.H. Fuhrhop, in Porphyrins and Metalloporphyrins, ed. K.M. Smith (Elsevier Sc. Publ. Comp., Amsterdam, 1975) p. 653.
- [23] A.T. Gradyushko and M.P. Tsvirko, Opt. Spectros. 31 (1971) 291.
- [24] R. van den Berg, private communication (1983).
- [25] R. van den Berg, H. van den Laan and S. Völker, submitted to Chem. Phys. Lett.
- [26] H.P.H. Thijssen and S. Völker, unpublished results (1985).
- [27] I. Coremans and R. van den Berg, unpublished results (1983).
- [28] R. Tamkivi, I. Renge and R. Avarmaa, Chem. Phys. Lett. 103 (1983) 103.

ABSTRACT

The temper
of free-base
(n-C₈) and
4.2 K. For the
PS, $T_{0\text{hom}} = T_0$
systems. The
measurements
in the n-octane
whether the ex
PS, $T_0^* (2xT_0)$
fact reached for

OPTICAL DEPHASING OF THE $S_1 \leftarrow S_0$ TRANSITION OF FREE-BASE
OCTAETHYLPORPHIN IN N-OCTANE AND POLYSTYRENE
STUDIED BY PHOTOCHEMICAL HOLE-BURNING.

A. Visser, R. van den Berg and S. Völker

ABSTRACT

The temperature dependence of holes burnt into the $S_1 \leftarrow S_0$ 0-0 transition of free-base octaethylporphin (OEP) in three sites of crystalline n-octane (n-C₈) and in amorphous polystyrene (PS) has been studied between 1.2 and 4.2 K. For the crystalline host, $\Gamma_{\text{hom}} - \Gamma_0 \propto \exp(-E/kT)$, with $E < 10 \text{ cm}^{-1}$. For PS, $\Gamma_{\text{hom}} - \Gamma_0 \propto T^{1.3 \pm 0.1}$, as previously found for other organic amorphous systems. The investigated T-regime, however, is too restricted, and measurements are planned to check a) whether the exponential dependence found in the n-octane crystal is also valid over a larger temperature range, and b) whether the expected extrapolation value of Γ_{hom} for $T \rightarrow 0$ in the amorphous PS, $\Gamma_0 = (2\pi T_1)^{-1} = 5.5 \text{ MHz}$, with T_1 the fluorescence lifetime of OEP, is in fact reached for this amorphous system.

1. INTRODUCTION

Optical dephasing processes in porphyrin molecules have so far only been studied by hole-burning in unsubstituted porphins (free-base porphin (H_2P) [5-14], free-base chlorin (H_2Ch) [11,15,16], Zn-porphin [17] and Mg-porphin [18]) incorporated either in n-alkane crystals or organic glasses, with the exception of a few cases like H_2 -phtalocyanine [1,2] and H_2 -tetra-4-tert.-butylphtalocyanine [3].

Since the homogeneous optical linewidth, Γ_{hom} , is always hidden under the inhomogeneous spectral band, it is only possible to get information on Γ_{hom} with special laser techniques either in the frequency or time domain. Hole-burning, which has been used in this work, belongs to the first category and can be summarized as follows: irradiation into the spectral absorption band with a narrow band laser of width $\Gamma_l \ll \Gamma_{hom}$ and frequency ν_0 can induce resonant molecules to undergo either a photochemical transformation, such that the product absorbs at a different frequency, or to pass over temporarily to a metastable state. This creates a hole in the original absorption line at frequency ν_0 . The hole may subsequently be probed with a scanning laser of low enough intensity to avoid burning the transition any further.

The hole, in essence, represents a negative replica of the homogeneous spectral transition and the holewidth, if carefully measured, yields the unknown quantity Γ_{hom} [5,6,9,13,19]. The photoproduct band or "anti-hole" will, in general, be broader than the hole because the laser selects molecules with a specific energy and not, necessarily, with the same environment. The relationship between transition energy and environmental parameters will be different for the photoproduct and the original molecules [20].

Systematic studies of holewidths in 0-0 and vibronic transitions of H_2P have been performed by varying the n-alkane crystalline host from n-hexane ($n-C_6$) to n-decane ($n-C_{10}$) [6-9,21]. However, no studies have been reported on a systematic variation of the guest molecule, from which one would also gain insight into guest-host interactions. In this work we have tried a first step in this direction. We have studied the temperature dependence of homogenous

linewidths of the $S_1 \leftarrow S_0$ transition of free-base octaethylporphyrin (OEP) in three sites of the crystalline host of n-octane ($n-C_8$), and in the amorphous host polystyrene (PS), between 1.2 and 4.2 K. As will be shown, an exponentially activated temperature dependence of Γ_{hom} is found for the crystalline host, as previously observed for unsubstituted porphyrins in n-alkanes [6,8,15,17,18,20]. Librational modes of much lower frequencies than in H_2P , however, seem to be responsible for the dephasing of OEP in n-octane.

We have further found that the homogeneous linewidth of OEP in PS follows a $T^{1.3}$ dependence, at least between 1.2 and 4.2 K. This result is not surprising, since a $T^{1.3}$ power law seems to be generally observed in organic glasses [10-13,16,19,22-24]. We have to emphasize that the results presented here are preliminary, and experiments down to 0.3 K and at least up to 20 K are planned in order to have a reliable interpretation of the data.

2. EXPERIMENTAL

Polycrystalline samples of OEP in n-octane ($n-C_8$) were obtained by directly dissolving OEP in the n-alkane. The solution was then cooled down to nitrogen temperature in a few minutes, and introduced in the cryostat at 4.2 K.

Amorphous samples of OEP in polystyrene (PS) were prepared by mixing a solution of OEP in ethanol with a solution of PS in toluene. A few drops of this mixture were placed on a glass plate, and the solvent was allowed to evaporate over several days. A transparent film with a thickness of about 0.1 mm was obtained. The sample was directly introduced in the ^4He -cryostat.

Holes were burnt with a single-frequency dye laser (Coherent, CR 599-21, amplitude stabilized to $< 0.5\%$ by an electro-optical modulator, with a dye mixture of rhodamine 6G and rhodamine B, scan range 30 GHz and frequency jitter < 2 MHz) as shown in fig. 1. In order to avoid power broadening and heating effects, burning powers of, respectively, $0.02-0.17 \mu\text{W}/\text{cm}^2$ in n-octane and $0.2-2.15 \mu\text{W}/\text{cm}^2$ in PS were used. Burning times were varied between 5 and 30 s. The holes were probed by scanning the same laser at reduced power

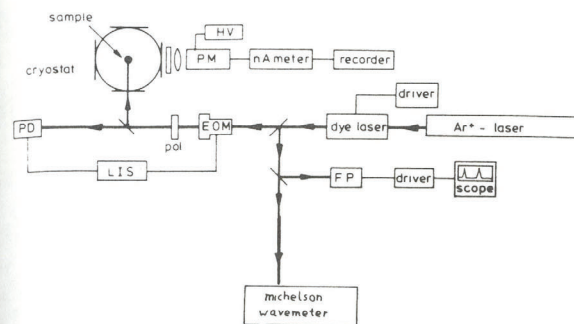


Fig. 1. Experimental set-up for PHB and NPHB, for details see text. FB: Fabry-Perot, PM: photomultiplier, EOM: electro-optic modulator, LIS: light intensity stabilizer, PD: photodiode.

(2-100x) over the spectral region of interest and simultaneously detecting the fluorescence signal. Only holes of relative depth $D < 5\%$ were taken for evaluation of the homogeneous linewidth, Γ_{hom} . The latter was determined from the relation $\Gamma_{\text{hom}} = \frac{1}{2}\Gamma_{\text{hole}} - \Gamma_1$, where Γ_{hole} is the measured holewidth extrapolated to the lowest burning fluences $P t$, and Γ_1 (≤ 2 MHz) is the frequency jitter of the laser [5].

The temperature in the cryostat between 1.2 and 4.2 K was controlled via the vapour pressure above the helium-bath and measured by a calibrated carbon resistor with an accuracy of ± 0.01 K.

3. RESULTS AND DISCUSSION

3.1 TEMPERATURE DEPENDENCE OF THE 0-0 TRANSITION OF OEP IN CRYSTALLINE N-OCTANE

Fig. 2 shows a broad band detected excitation spectrum of the $S_1 \leftarrow S_0$ 0-0 region of octaethylporphyrin (OEP) in n-octane ($n\text{-C}_8$) at 4.2 K. Holes were subsequently burnt in the K_2 , L_1 and M_2 sites between 1.2 and 4.2 K.

Fig. 3a is a plot of the homogeneous linewidth, Γ_{hom} , versus temperature T between 1.2 and 4.2 K for two sites, K_2 and M_2 , of the 0-0 transition of OEP in $n\text{-C}_8$. Notice that Γ_{hom} extrapolates to a value of 5.4 MHz when $T \rightarrow 0$, which corresponds to the fluorescence lifetime-limited value $(2\pi T_1)^{-1}$ of OEP ($T_1 = 29.5$ ns [4]). The third site, L_1 , did not broaden between 1.2 and 4.2 K. The measured width, $\frac{1}{2}\Gamma_{\text{hole}} = 9$ MHz, was larger than the expected value of Γ_0 . The origin of this discrepancy is not known yet, and measurements at $T > 4.2$ K and $T < 1.2$ K are planned.

In fig. 3b we have plotted the data of fig. 3a in a $\log(\Gamma_{\text{hom}} - \Gamma_0)$ versus $(T)^{-1}$ form. The slopes of these curves yield activation energies $E = 3.1 \pm 0.4$ cm^{-1} and 7.0 ± 0.3 cm^{-1} for the K_2 and M_2 sites respectively. The results, however, are preliminary since the measured temperature regime was very restricted. We interpret the results in terms of very low frequency librational modes of OEP in $n\text{-C}_8$. It is surprising that these energies are much lower than those found for H_2P in the B-site (15 cm^{-1}) and the A-site

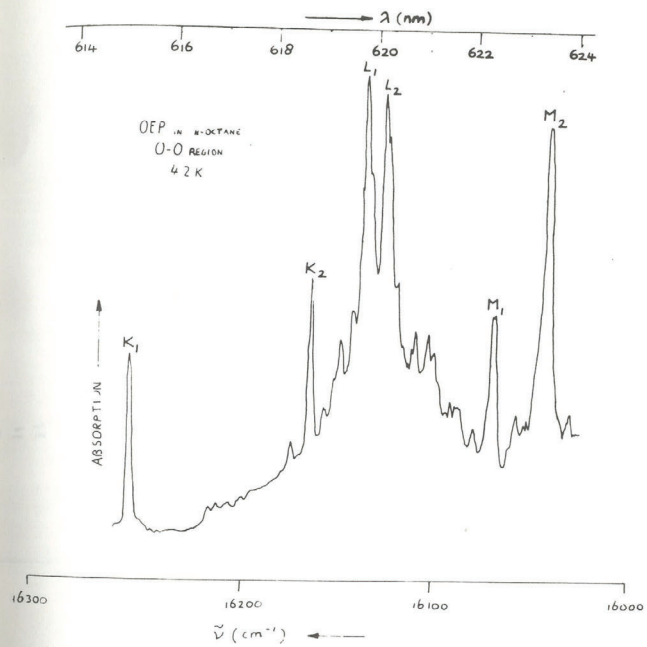


Fig. 2. Broad band detected fluorescence excitation spectrum of the $S_1 \leftarrow S_0$ transition of OEP in crystalline n-octane at 4.2 K. The principal sites have been called K, L and M.

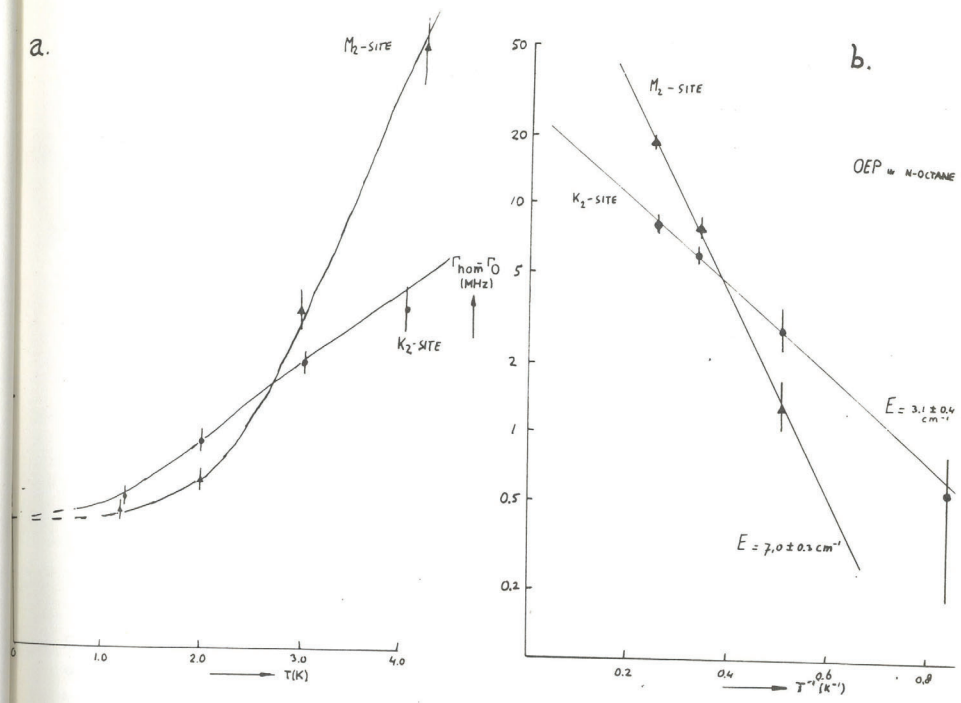


Fig. 3.a. Temperature dependence of the homogeneous linewidth Γ_{hom} of the $S_1 + S_0$ 0-0 transition of OEP in n-octane for the sites K_2 and M_2 .
 b. Increase of the homogeneous linewidth, $(\Gamma_{\text{hom}} - \Gamma_0)$, as a function of the inverse of the temperature for the same sites as in fig. 3a.

($\sim 30 \text{ cm}^{-1}$) of n-C₈ [6]. In the latter case, however, the guest molecule is smaller (an unsubstituted porphin) and it is known that the value of the librational frequency or pseudo-localized phonon mode depends strongly on the guest-host interaction [6-9]. Thus, the size of the substitutional cage in which the guest is incorporated plays a fundamental role in the dephasing process.

With this picture in mind, we imagine that OEP needs a larger substitutional cage than H₂P and, therefore, probably replaces one more chain of n-C₈ as compared to the latter. As a consequence, the guest molecule has a looser fit, which leads to lower librational frequencies. In order to be able to interpret the data in a reliable way, experiments over a more extended temperature region will be performed. We would further expect that the third site L₁, which did not show any broadening up to 4.2 K, will dephase with a larger activation energy. Site L₁ has probably a tighter fit than the K₂ and M₂ sites in the n-C₈ host.

3.2 TEMPERATURE DEPENDENCE OF THE 0-0 TRANSITION OF OEP IN AMORPHOUS POLYSTYRENE

Holes were burnt on the red wing of the 0-0 transition of octaethylporphin (OEP) in polystyrene (PS) at 619.7 nm. Fig. 4a is a plot of $\frac{1}{2}\Gamma_{\text{hole}}$ versus T between 1.2 and 4.2 K. Notice that the values of $\frac{1}{2}\Gamma_{\text{hole}}$ extend from ~ 1 GHz at 4 K down to ~ 0.2 GHz at 1 K. The data seem to extrapolate smoothly to $\Gamma_0 = 0$ GHz on the scale of the plot, which is consistent with the expected fluorescence lifetime-limited value of OEP, $\Gamma_0 = 5.4$ MHz [4]. Experiments down to 0.3 K, which are planned, should yield values of $\frac{1}{2}\Gamma_{\text{hole}}$ of ~ 40 MHz.

A log-log plot of $(\Gamma_{\text{hom}} - \Gamma_0)$ versus T of the same data as in fig 4a is given in fig. 4b. As previously found for many organic glassy systems [10-13,16,19,22-24], OEP also shows a $T^{1.3 \pm 0.1}$ dependence. If we compare our values of $\Gamma_{\text{hom}} - \Gamma_0$ with those of Gorokhovskii et al. [4] in the same temperature regime (see the three points at 1.0, 1.2 and 1.6 K in fig. 4b), we

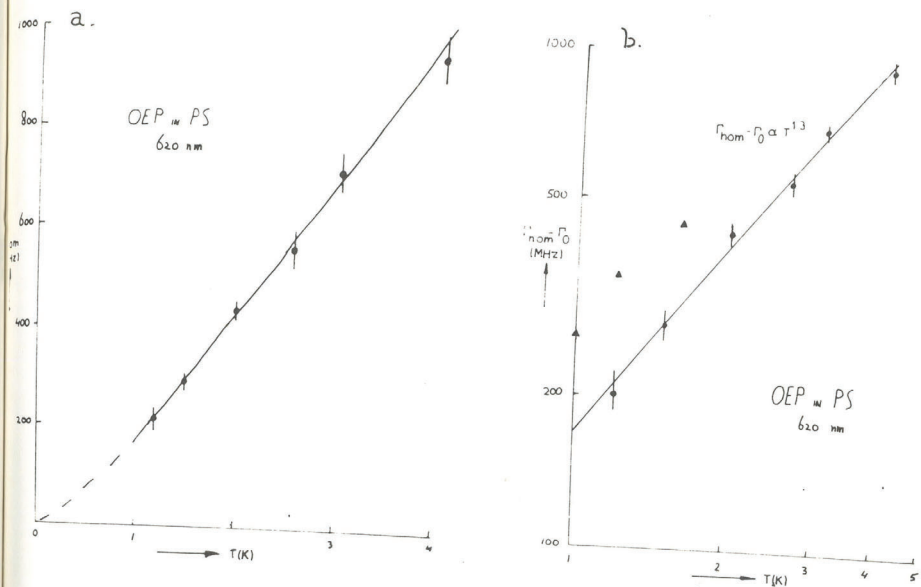


Fig. 4.a. Temperature dependence of the homogenous linewidth, Γ_{hom} of the 0-0 transition of OEP in polystyrene (PS). Holes were burnt at 620 nm.

b. Log-log plot of $\Gamma_{\text{hom}} - \Gamma_0$ versus T for OEP in PS. The solid circles represent our data between 1.2 and 4.2 K, which follow a $T^{1.3}$ power law. The solid triangles are reproduced from hole-burning data taken from the literature [4].

observe that they differ by a factor of about 1.5. The reason for this difference is probably due to the fact that the holes reported in ref. [4] were probed in transmission through the sample. Such a detection method usually yields somewhat broader holes than fluorescence excitation spectroscopy for a given burning fluence [19]. The T-dependence of $\Gamma_{\text{hom}} - \Gamma_0$ between 0.3 and 1.2 K found by Gorokhovskii et al. [4] is the same as previously found by us for many amorphous systems. However, below 0.3 K and down to 0.05 K the T-dependence of ref. [4] crosses over from $\sim T^{0.6} - T^{0.8}$ (between 0.4 and 0.09 K) to $T^{1.7} - T^{1.5}$ (between 0.09 and 0.05 K). Whether such kinks in the T-dependence are physically real, has still to be verified. We are planning measurements on this system down to 0.3 K to check whether a smooth T-dependence, as we would expect, extrapolates to $\Gamma_0 = (2\pi T_1)^{-1}$, and up to at least 20 K to check over which T-regime over which the $T^{1.3}$ power law is valid [25].

ACKNOWLEDGEMENTS

We would like to thank H. van der Laan for his assistance with the measurements. The investigations were supported by the Netherlands Foundation for Physical Research (F.O.M.) with financial aid from the Netherlands Organization for the Advancement of Pure Research (Z.W.O.).

REFERENCES

- [1] A. Gutierrez, G. Castro, G. Schulte and D. Haarer in: Electronic Excitations and Interaction Processes in Organic Molecular Aggregates, eds. P. Reineker, H. Haken and H.C. Wolf (Springer Verlag, Berlin, 1983) p.206.
- [2] H.W.H. Lee, A.L. Huston, M. Gehrtz and W.E. Moerner, Chem. Phys. Lett. 144 (1985) 491.
- [3] A.A. Gorokhovskii, J.V. Kikas, V.V. Palm and L.A. Rebane, Sov. Phys. Sol. State 23 (1981) 602.

- [4] A.A. Gorokhovskii, V. Korrovits, V.V. Palm and M. Trummal, Chem. Phys. Lett. 125 (1986) 355.
- [5] S. Völker, R.M. Macfarlane, A.Z. Genack, H.P. Trommsdorff and J.H. van der Waals, J. Chem. Phys. 67 (1977) 1759.
- [6] S. Völker, R.M. Macfarlane and J.H. van der Waals, Chem. Phys. Lett. 53 (1978) 8.
- [7] S. Völker and R.M. Macfarlane, Chem. Phys. Lett. 61 (1979) 421.
- [8] A.I.M. Dicker, J. Dobkowski and S. Völker, Chem. Phys. Lett. 84 (1981) 415.
- [9] A.I.M. Dicker and S. Völker, Chem. Phys. Lett. 87 (1982) 481.
- [10] H.P.H. Thijssen, A.I.M. Dicker and S. Völker, Chem. Phys. Lett. 92 (1982) 7.
- [11] H.P.H. Thijssen, R. van den Berg and S. Völker, Chem. Phys. Lett. 97 (1983) 295.
- [12] H.P.H. Thijssen, R. van den Berg and S. Völker, Chem. Phys. Lett. 103 (1983) 23.
- [13] H.P.H. Thijssen and S. Völker, Chem. Phys. Lett. 120 (1985) 496.
- [14] H.P.H. Thijssen and S. Völker, J. Chem. Phys. 85 (1986) 785.
- [15] S. Völker and R.M. Macfarlane, J. Chem. Phys. 73 (1980) 4476.
- [16] F.A. Burkhalter, G.W. Suter, U.P. Wild, U.D. Samoilenko, N.V. Rasumova and R.I. Personov, Chem. Phys. Lett. 94 (1983) 483.
- [17] R.M. Shelby and R.M. Macfarlane, Chem. Phys. Lett. 64 (1979) 545.
- [18] A.I.M. Dicker (1985), L.W. Johnson, S. Völker and J.H. van der Waals, Chem. Phys. Lett. 100 (1983) 8.
- [19] R. van den Berg and S. Völker, Chem. Phys. Lett. 127 (1986) 525.
- [20] S. Völker and R.M. Macfarlane, IBM J. Res. Dev. 23 (1979) 547.
- [21] R.M. Macfarlane and S. Völker, Chem. Phys. Lett. 69 (1980) 151.
- [22] H.P.H. Thijssen, S. Völker, M. Schmidt and H. Port, Chem. Phys. Lett. 94 (1983) 537.
- [23] J. Fünfschilling and I. Zschokke-Gränacher, Chem. Phys. Lett. 110 (1984) 315.
- [24] L.W. Molenkamp and D.A. Wiersma, J. Chem. Phys. 83 (1985) 1.

[25] R. van den Berg, A. Visser and S. Völker, chapter 3 of this report (to be submitted for publication).

SPECTRAL HOLE-BURNING IN ORGANIC GLASSES.
A STUDY OF RESORUFIN AND FREE-BASE PORPHIN BETWEEN 0.3 AND 20 K

R. van den Berg, A. Visser and S. Völker.

ABSTRACT

Spectral holes have been burnt in the $S_1 \leftarrow S_0$ 0-0 transition of resorufin in polymethylmethacrylate (PMMA) and glycerol, and free-base porphin (H_2P) in PMMA and polyethylene (PE) between ~ 0.3 and ~ 20 K. The holewidths follow a $T^{1.3}$ dependence over almost two decades in temperature and extrapolate to the fluorescence lifetime-limited value, $\Gamma_0 = (2\pi T_1)^{-1}$, of each guest for $T \rightarrow 0$. The dependence of the holewidth on laser burning fluence for resorufin in glycerol is used to explain the discrepancy between recently reported hole-burning data. A discussion is given on the differences between photon echo and hole-burning experiments. The results have been fitted with a model for optical dephasing.

1. INTRODUCTION

Most of the optical dephasing studies on organic glasses have been performed by means of spectral hole-burning [1-15], and it has only been recently that photon echoes were used to measure homogeneous linewidths in organic amorphous materials [16-18]. In general, these techniques may yield different physical quantities, because they measure on different time scales. In fact, it has been claimed that optical linewidths of resorufin in ethanol [17] and in glycerol [18] were different when measured with the hole-burning technique as compared to ps two-pulse photon echoes, and it was concluded from these experiments that holes do not reflect the homogeneous linewidths.

Furthermore, although for a wide variety of organic systems a $T^{1.3}$ temperature dependence of the homogeneous linewidth, Γ_{hom} , was found [5-10,13-16,19], the temperature regime over which such a behaviour was observed was relatively narrow, in many cases only between 1.2 and 4.2 K [5,7a,8,10a,15,17]. In other systems it was extended down to 0.3 K [6,7b,c,9,10b,13]. Above 4.2 K only a few hole-burning data are reported which show a $T^{1.3}$ dependence of Γ_{hom} : H₂P in glycerol:ethanol (10:1) up to 20 K [5] and tetracene in diphenyl- and dimethyl-anthracene up to 11 K [14]. Also accumulated photon echoes on pentacene in PMMA between 1.5 and 12 K [16] reveal a $T^{1.3}$ power law. Exceptions, however, are the two-pulse photon echo data of resorufin in ethanol [17] and glycerol [18] mentioned above, which show deviations from the $T^{1.3}$ dependence for temperature above 4.2 K and up to 11.4 and 25.5 K respectively.

In order to clear up the validity of the $T^{1.3}$ power law, we studied the $S_1 \leftarrow S_0$ 0-0 transitions of various organic molecules in amorphous hosts by means of hole-burning between ~ 0.3 and ~ 20 K: resorufin in polymethylmethacrylate (PMMA) and glycerol, and free-base porphyrin (H₂P) in PMMA and polyethylene (PE). As will be shown, our hole-burning results yield again a $T^{1.3}$ law over almost two decades in temperature, which seems to confirm the "universality" of the T-dependence of Γ_{hom} at low temperatures.

From a study of the holewidth dependence on laser burning power and

burning time of resorufin in glycerol it is possible to understand the discrepancy between the holewidths measured by us and those recently reported in the literature [18] for the same system. In contrast, discrepancies between the photon echo data [18] and our hole-burning data as a function of temperature cannot be explained by spectral diffusion in terms of the formalism given in ref. [18].

A fit of a model for optical dephasing [20] to our experimental results between 0.3 and 20 K indicates that very low frequency modes in addition to two-level-systems (TLS) of the glass may be responsible for the optical dephasing in these systems. The activation energy estimated by us for resorufin in glycerol ($E \sim 6 \text{ cm}^{-1}$) is much smaller than that reported in ref. [18] ($E = 37 \text{ cm}^{-1}$). No experimental evidence for such low frequency modes, however, has been found yet.

2. EXPERIMENTAL

Two samples of resorufin (Janssen Chimica) in glycerol were prepared with optical densities of 0.2 and 0.6 at 580 nm respectively. Samples of resorufin and free-base porphin (H_2P) in PMMA (with optical densities of respectively 0.4 at 578 nm and 6.10^{-3} at 610 nm) were prepared by mixing solutions of the guest molecules in ethanol, with PMMA dissolved in dichloromethane. After pumping in an oven at 60 °C for three days, transparent films of PMMA were obtained with a thickness of 100 μm for resorufin and 190 μm for H_2P . Free-base porphin in PE (Wacker, high density $\rho = 0.955 \text{ g/ml}$) at $c = 10^{-4} - 10^{-5} \text{ mol/l}$ was prepared by adding a solution of H_2P in MTHF to molten PE. This mixture was kept above the melting point of PE (135 °C) until the MTHF was evaporated. The sample was subsequently cooled down to room temperature in about one hour.

Holes were burnt with a single frequency dye laser (Coherent, model CR 599-21, amplitude stabilized to $< 0.5 \%$ by an EO-modulator, with

rhodamine 6G, scan range 30 GHz, frequency jitter < 2 MHz). In order to burn holes of relative depth $D \sim 2-3\%$, different burning fluences, $P t$ (P : laser power, t : burning time) were used. These values, which depend on the sample and increase with temperature, are given in table 1. The laser was focused on an area of $\sim 7 \text{ mm}^2$, and its power was controlled with a variable beam attenuator (NRC, model M 928-B) and neutral density filters. The holes were probed by scanning the laser, attenuated by a factor of 5-100, over the spectral region of the hole, and detecting the fluorescence signal (at $\lambda > 610 \text{ nm}$ for resorufin, and at $\lambda > 645 \text{ nm}$ for H_2P) with a cooled photomultiplier (EMI, model 9658 R). The holes burnt in resorufin in glycerol were probed simultaneously by means of the fluorescence signal and the transmission signal through the sample (the latter was detected with a photodiode, EG&G, model HUV 4000). The holewidths of resorufin in glycerol at a given temperature were independent of the cooling rate of the sample, in contrast with those of resorufin in ethanol [10b].

The homogeneous linewidth, Γ_{hom} , was determined from the relation $\Gamma_{\text{hom}} = \frac{1}{2}\Gamma_{\text{hole}} - \Gamma_1$ where Γ_{hole} is the measured holewidth extrapolated to the lowest burning fluences $P t$, and Γ_1 is the frequency jitter of the laser ($\Gamma_1 \leq 2 \text{ MHz}$).

Between 1.2 and 4.2 K a conventional bath cryostat was used in which the temperature, varied by means of the vapour pressure, was measured both by this pressure and by a calibrated carbon resistor with an accuracy of $\pm 0.01 \text{ K}$. For temperatures below 1.2 K, a ^3He -glass insert was placed inside the ^4He -bath cryostat [21]. After pumping the ^4He -bath to 1.2 K, ^3He was condensed into the inner cryostat, where it could be kept liquid for $\sim 3-5$ hours. By reducing the vapour pressure, temperatures down to 0.3 K were reached. The temperature was measured by a calibrated carbon resistor (Matsushita 100 Ω , 1/8 W) placed in contact with the sample and, simultaneously, via the vapour pressure. The accuracy in the temperature determination was estimated to vary between $\pm 0.01 \text{ K}$ and $\pm 0.02 \text{ K}$ [7b,8,9,21].

Between 4.2 and 22 K a gas flow cryostat (Leybold-Heraeus) was used in which the temperature of the gas flow was stabilized by an electronic unit. The latter measures the resistance of a thermistor and controls the electric

Table 1. Laser burning fluence $P t$ ($\mu\text{J}/\text{cm}^{-2}$) used for various organic systems at different organic amorphous at different temperatures.

Sample	T (K)	$P t$ ($\mu\text{J}/\text{cm}^{-2}$)
Resofin/glycerol	0.4	0.6
	22	250
Reso/PMMA	1.2	1.3
	11.1	62
$\text{H}_2\text{P}/\text{PMMA}$	0.3	20
	13.4	1300
$\text{H}_2\text{P}/\text{PE}$	0.3	-2
	16.8	250

current through a heater [22] In this cryostat the temperature is measured close to the sample (but not in direct contact with it) by a calibrated carbon resistor, via a Wheatstone bridge. The accuracy of the temperature given by the resistor is ± 0.02 K.

3. RESULTS AND DISCUSSION

In fig. 1 a log-log plot of $\Gamma_{\text{hom}} - \Gamma_0$ versus temperature is given for resorufin in PMMA (open triangles) and glycerol (open squares) and for H₂P in PMMA (closed circles) and PE (open circles). Holes were burnt in these samples at the red wing of their 0-0 absorption band at about 591 nm for resorufin, and at 610 nm and 615 nm for H₂P in PMMA and PE respectively. All four curves follow a power law dependence, $\Gamma_{\text{hom}} - \Gamma_0 \propto T^{1.3 \pm 0.1}$, over almost two decades in temperature (from ~ 0.3 to ~ 20 K), independent of the guest and the host, and independent of the hole-burning mechanism (which is intra-molecular for H₂P and inter-molecular between the guest and the host for resorufin). These results confirm the general behaviour observed previously by us in organic glassy systems [5-10], the validity of which has now been extended to a wider temperature regime.

Fig. 2 is a plot of the homogeneous linewidth, Γ_{hom} , as a function of temperature for resorufin in PMMA [7c], glycerol and PE [7d], and for H₂P in PMMA and PE [9]. Only data at temperatures below 1.2 K are shown in the figure. Notice that the three curves of resorufin and both curves of H₂P extrapolate to a value Γ_{hom} for $T \rightarrow 0$ which is determined by the fluorescence lifetime T_1 of each guest, $\Gamma_0 = (2\pi T_1)^{-1}$. We have found that $\Gamma_0 = 10$ MHz for H₂P [25] and $\Gamma_0 = 20$ MHz for resorufin [7c]. It should be remarked that the value of Γ_0 obtained by us for resorufin is markedly smaller than that reported by Fayer and co-workers for the same molecule, $\Gamma_0 = 46.8$ MHz, which corresponds to a fluorescence decay time of 3.4 ns [18].

The dependence of the holewidth, $\frac{1}{2}\Gamma_{\text{hole}}$, as a function of burning time

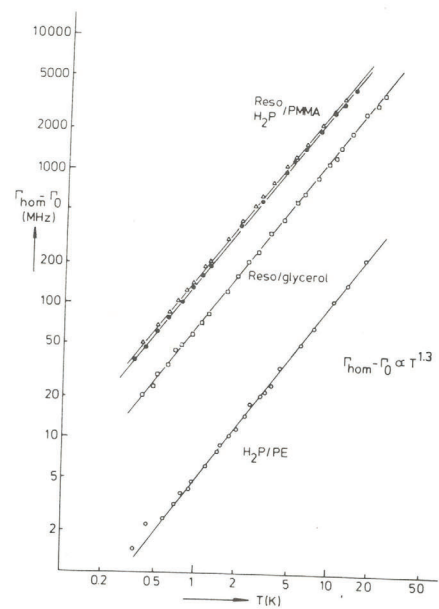


Fig. 1. Log-log plot of $\Gamma_{\text{hom}} - \Gamma_0$ versus T for resorufin in PMMA (open triangles), H_2P in PMMA (closed circles), resorufin in glycerol (open squares) and H_2P in PE (open circles). The data follow $\Gamma_{\text{hom}} - \Gamma_0 \propto T^{1.3}$ between ~ 0.3 and ~ 20 K.

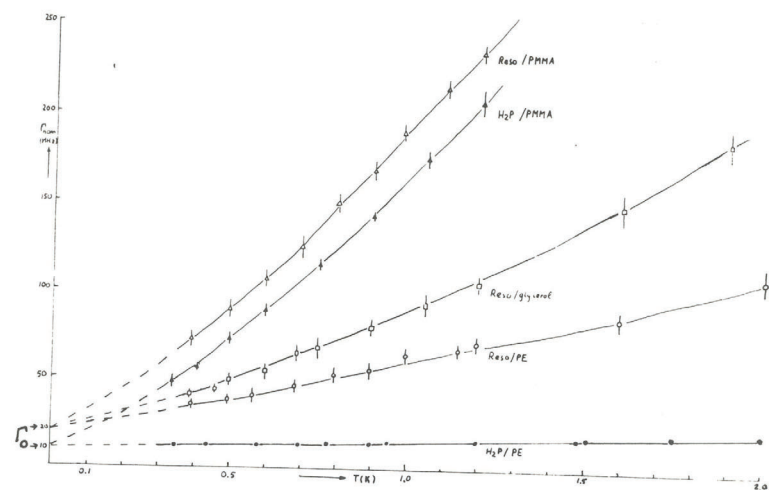


Fig. 2. Temperature dependence of Γ_{hom} of the 0-0 transition of resorufin in PMMA, H₂P in PMMA, resorufin in glycerol, resorufin in PE and H₂P in PE between -0.3 and 2.0 K. Notice that the value of Γ_{hom} extrapolates or reaches the fluorescence-limited value of each guest molecule, $\Gamma_0 = (2\pi T_1)^{-1}$, for $T \rightarrow 0$.

for resorufin in glycerol is shown in fig. 3a for two different burning powers at $T = 1.2$ K. The holes burnt at higher power ($1.6 \mu\text{W}/\text{cm}^2$) were probed by monitoring simultaneously the fluorescence signal at 90° from the excitation direction (open triangles) and the transmission signal through the sample (closed triangles). Holes burnt at lower power ($0.27 \mu\text{W}/\text{cm}^2$) were detected in fluorescence only (open circles). Notice that all curves extrapolate to $\frac{1}{2}\Gamma_{\text{hole}} = \Gamma_{\text{hom}} = 105$ MHz when $t \rightarrow 0$, although the two upper curves reach the same value with a much steeper slope. A similar effect was previously observed by us for a non-photochemical hole-burning (NPHB) system, pentacene in PMMA [10a]. Two conclusions can be drawn from these results: first, the true value of Γ_{hom} at a given temperature is only reached at the lowest possible laser fluences; second, for a given laser burning power, holes detected in transmission through the sample are broader than those detected in fluorescence, and only at very short burning times they coincide (in the case of resorufin in glycerol this occurs at $t < 2$ s for $P = 1.6 \mu\text{W}/\text{cm}^2$).

The data of the fluorescence and transmission curves of fig. 3a, together with some additional values of $\frac{1}{2}\Gamma_{\text{hole}}$, were used in fig. 3b in the form of a log-log plot of $\frac{1}{2}\Gamma_{\text{hole}}$ versus laser fluence, $P t$. All data fall on two straight lines (upper one for holes detected in transmission, lower one for holes probed in fluorescence), which obey a power law dependence of $P t$, $\frac{1}{2}\Gamma_{\text{hole}} = c (P t)^{0.23 \pm 0.01}$. This $(P t)^{0.23}$ power law seems to be valid for $P t > 1.4 \mu\text{J}/\text{cm}^2$ and up to $3.5 \text{ mJ}/\text{cm}^2$, thus over at least three decades in $P t$ values. The same $P t$ dependence of $\frac{1}{2}\Gamma_{\text{hole}}$ was found by us for pentacene in PMMA [10a] and other organic glasses [24]. It differs from a square root dependence on power expected from simple saturation broadening effects [25,26].

It should be remarked that the absolute values of $P t$ needed to burn resorufin in glycerol are $\sim 10^4 - 10^5$ times smaller than those needed for pentacene in PMMA. Since the optical densities of both samples were similar (0.6 and 0.9 respectively), we conclude that the hole-burning efficiency for resorufin is orders of magnitude larger than that for pentacene. This suggests that photochemical hole-burning (PHB) takes place in the ionic dye resorufin [7c], in contrast to non-photochemical hole-burning (NPHB) assumed

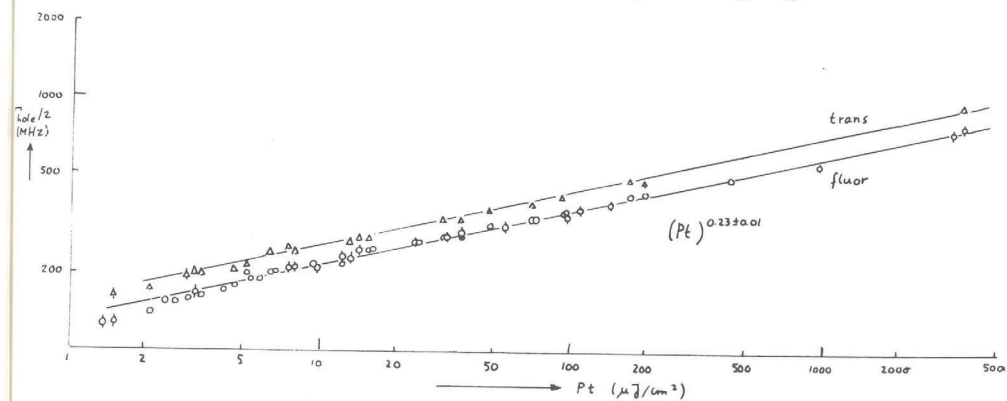
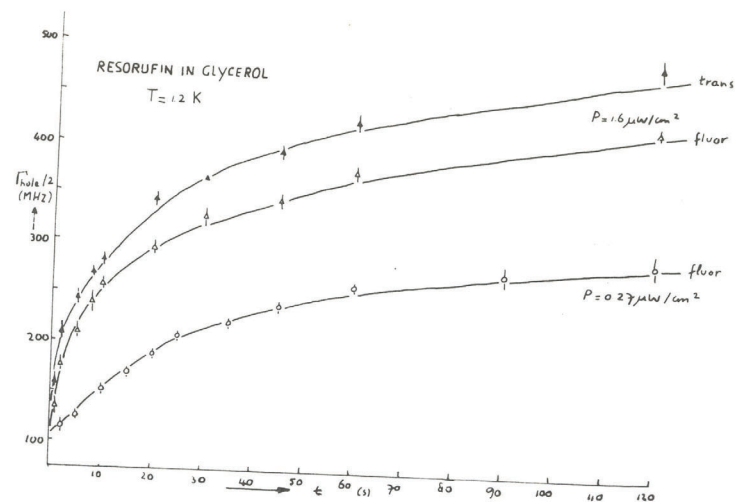


Fig. 3.a. $\frac{1}{2}\Gamma_{\text{hole}}$ as a function of burning time t for resorufin in glycerol, at 1.2 K for two burning powers. At $P = 1.6 \mu\text{W}/\text{cm}^2$ the holes were probed simultaneously via fluorescence excitation signal and the transmission signal through the sample. For $t \rightarrow 0$, $\frac{1}{2}\Gamma_{\text{hole}} = \Gamma_{\text{hom}} = 105 \text{ MHz}$.

b. Log-log plot of $\frac{1}{2}\Gamma_{\text{hole}}$ versus burning fluence Pt for resorufin in glycerol at 1.2 K. Holes were probed in transmission (upper curve) and fluorescence excitation (lower curve). The data follows $\frac{1}{2}\Gamma_{\text{hole}} = c (Pt)^{0.23 \pm 0.01}$ for $Pt > 1.4 \mu\text{J}/\text{cm}^2$ (at least up to $3.5 \text{ mJ}/\text{cm}^2$).

to occur in pentacene [10a,16]. Further we should notice that P t-values used for H₂P (which undergoes PHB) in PMMA and ethanol are of the same order as those used for resorufin in the same two hosts (for similar O.D.values), which supports a PHB-mechanism for resorufin.

In fig. 4 we have plotted $\log(\Gamma_{\text{hom}} - \Gamma_0)$ versus $\log T$ for the 0-0 transition of resorufin in glycerol, with $\Gamma_0 = 20$ MHz. The top (open triangles) and bottom (closed triangles) curves are data taken from recent hole-burning (between 1.7 and 25.5 K) and photon echo (between 1.1 and 21 K) experiments by Fayer and co-workers [18]. The middle curve (open circles) represents our hole-burning data measured at 588 nm between 0.4 and 22 K. As mentioned already in fig. 1, the curve follows a $T^{1.3}$ dependence over almost two decades in temperature. This is not the case for the data of ref. [18], where both hole-burning and photon echoes show a strong deviation from a $T^{1.3}$ power law.

When comparing our hole-burning data to those of ref. [18] we notice that for $T \leq 2$ K our holewidths are a factor of about three narrower. This discrepancy can be understood phenomenologically in terms of burning fluences with help of fig. 3b. The value of $12 \mu\text{J}/\text{cm}^2$ at 1.7 K reported in ref. [18] for holes probed in transmission is about a factor of ten larger than that used by us at the same temperature for holes probed in fluorescence. Notice in fig. 3b that a P t value of $12 \mu\text{J}/\text{cm}^2$ yields a holewidth $\frac{1}{2}\Gamma_{\text{hole}}$ of ~ 270 MHz at 1.2 K, which is very similar to that one would obtain when extrapolating the data of ref. [18] to 1.2 K ($\frac{1}{2}\Gamma_{\text{hole}} = 300$ MHz). The same argument is valid for data at high temperatures: at 25.5 K a fluence of $7.5 \text{ mJ}/\text{cm}^2$ was reported [18], whereas we only used $250 \mu\text{J}/\text{cm}^2$ at 22 K.

Notice further in fig. 4 that the values of $\Gamma_{\text{hom}} - \Gamma_0$ at 1.1 K and at ~ 10 -12 K obtained by us from hole-burning experiments are very similar to those obtained by photon echoes [18], but they deviate from each other for $1.1 < T < 10$ K and for $T > 12$ K. Whether this discrepancy has a physical meaning, or is caused by some experimental artifact, we cannot say. If we assume, for the moment, that the photon echo data Γ_{PE} [18] yield the true values of Γ_{hom} and that the contribution of the extra broadening observed in our hole-burning data Γ_{HB} would be due to spectral diffusion, then it is easy

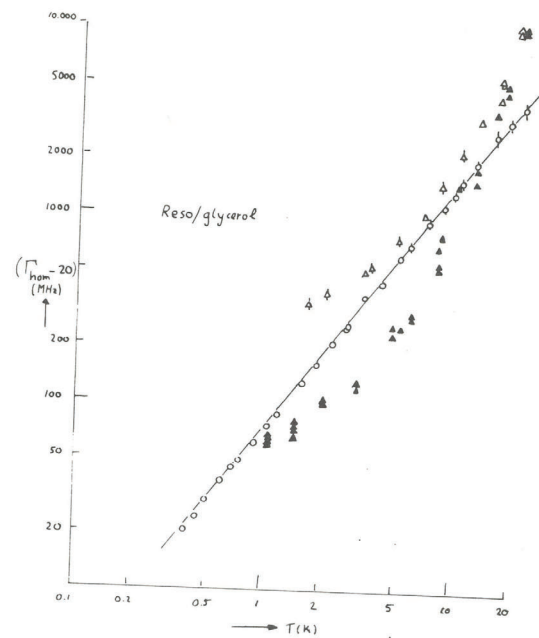


Fig. 4. Log-log plot of $\Gamma_{\text{hom}} - \Gamma_0$ versus T for resorufin in glycerol between ~ 0.3 and ~ 20 K. $\Gamma_0 = 20$ MHz. The upper (open triangles) and lower (closed triangles) data were taken from ref. [18]. The middle curve (open circles) represents our hole-burning data, which follows $\Gamma_{\text{hom}} - \Gamma_0 \propto T^{1.3 \pm 0.1}$ between ~ 0.3 and 22 K.

to verify that this extra broadening does not obey a simple power law dependence on temperature, $\Gamma_{\text{HB}} - \Gamma_{\text{PE}} \propto T^\alpha$, as claimed by Fayer and coworkers [18]. Preliminary transient hole-burning experiments on H₂P in PE between 1.2 and 4.2 K performed by us on a time scale of ms [27] yielded the same results as those obtained in a conventional way in the time scale of minutes, from which we conclude that spectral diffusion is not observed for this amorphous systems in between these two time scales.

If we assume, on the other hand, that our hole-burning data do reflect the homogeneous linewidth for resorufin in glycerol (without spectral diffusion contribution), then it is possible to try to fit the experimental values with a theoretical model. As recently done for resorufin in ethanol [10b] and previously for various other organic amorphous systems [9], we have applied Jackson and Silbey's model [20] in its simplest form:

$$\Gamma_{\text{hom}} - \Gamma_0 = aT + b \frac{\exp(-E/kT)}{1 - \exp(-E/kT)}, \quad (1)$$

where the first term represents the contribution of two-level system (TLS) of the glass to the dephasing, and the second term is due to librational motion of the guest in the host. We have assumed that at $T \approx 0.4$ K only the first term in eq. (1) plays a role. Thus we can estimate the value of $a = 60$ MHz/K. From the best fit of eq. (1) to the data of resorufin in glycerol between 0.4 and 22 K, we have obtained a value of $E = 6.0 \pm 0.3 \text{ cm}^{-1}$, which is much smaller than the value of 37 cm^{-1} reported in ref. [18]. By using eq. (1) it is impossible to fit our data with $E = 37 \text{ cm}^{-1}$. We have also tried to fit the data with a different first term, namely cT^α , as used by Fayer et al. in ref. [18]. In this case, and allowing for a variation in α ($1 \leq \alpha \leq 2$), we have obtained a best fit with $\alpha = 1.2$ and $E = 6.3 \text{ cm}^{-1}$, which is very similar to the value of E obtained with $\alpha = 1$.

The fits for the other samples (see fig. 1) yielded values of $E = 2.6 \pm 0.3 \text{ cm}^{-1}$ for resorufin in PMMA, and $E = 2.5 \pm 0.1 \text{ cm}^{-1}$ for H₂P in PMMA, which are similar to those found previously for the same samples, but were measured in the restricted T-regime between 0.3 and 4.2 K [9]. The activation

energy for H_2P in PE, in contrast, varies from $E = 7 \text{ cm}^{-1}$ to $E = 12 \text{ cm}^{-1}$, depending on the value chosen for α ($1 \leq \alpha \leq 1.2$). Since there is no spectroscopic evidence for librational modes with these energies from site-selection or hole-burning experiments [9], we looked for a correlation between E-values and spectral distances δ between hole and phonon-sidehole. The values for δ for the various samples studied are: $\delta = 26 \pm 1 \text{ cm}^{-1}$ for resorufin in glycerol, $\delta = 14 \pm 3 \text{ cm}^{-1}$ for resorufin in PMMA and $\delta = 12 \pm 2 \text{ cm}^{-1}$ for the H_2P in PMMA and in PE. Thus, no direct correlation seems to exist between E-values and hole-phonon sidehole frequency differences.

4. CONCLUSIONS

The hole-burning results presented here for four organic amorphous systems measured between 0.3 and 20 K have shown that $\Gamma_{\text{hom}} - \Gamma_0 \propto T^{-1.3}$ over almost two decades in temperature. For the system resorufin in glycerol the holewidths at 1.2 K are a factor of ~ 3 smaller than those reported in the literature [18]. An explanation for this discrepancy has been given. The data were fitted with a theoretical model for optical dephasing from which activation energies $E \leq 12 \text{ cm}^{-1}$ resulted. The value of E for resorufin in glycerol, $E = 6.0 \pm 0.3 \text{ cm}^{-1}$, is much smaller than that claimed in ref. [18]. The difference between our hole-burning data and the photon echo data of ref. [18] cannot be interpreted in terms of spectral diffusion following a power law dependence on temperature.

ACKNOWLEDGEMENTS

We would like to thank M.D. Fayer for sending us preprints on his photon echo results on resorufin in glycerol. The investigations were supported by the Netherlands Foundation for Physical Research (F.O.M.) with financial aid from the Netherlands Organization for the Advancement of Pure Research (Z.W.O.).

REFERENCES

- [1] J.M. Hayes, R.P. Stout and G.J. Small, *J. Chem. Phys.* 74 (1981) 4266.
- [2] E. Cuellar and C. Castro, *Chem. Phys.* 54 (1981) 217.
- [3] A.A. Gorokhovskii, J.V. Kikas, V.V. Palm, and L.A. Rebane, *Sov. Phys. Solid State* 23 (1981) 602.
- [4] J. Friedrich, H. Wolfrum and D. Haarer, *J. Chem. Phys.* 77 (1982) 2309.
- [5] H.P.H. Thijssen, A.I.M. Dicker and S. Völker, *Chem. Phys. Lett.* 92 (1982) 7.
- [6] H.P.H. Thijssen, S. Völker, M. Schmidt and H. Port, *Chem. Phys. Lett.* 94 (1983) 537.
- [7] a. H.P.H. Thijssen, R. van den Berg and S. Völker, *Chem. Phys. Lett.* 97 (1983) 295; b. 103 (1983) 23; c. 120 (1983) 503.
- [8] H.P.H. Thijssen and S. Völker, *Chem. Phys. Lett.* 120 (1985) 496.
- [9] H.P.H. Thijssen and S. Völker, *J. Chem. Phys.* 85 (1986) 785.
- [10] a. R. van den Berg and S. Völker, *Chem. Phys. Lett.* 127 (1986) 525; b. 137 (1987) 201.
- [11] F.A. Burkhalter, G.W. Suter, U.P. Wild, U.D. Samoilenko, N.V. Rasumova and R.I. Personov, *Chem. Phys. Lett.* 94 (1983) 483.
- [12] T.P. Carter, B.L. Fearey, J.M. Hayes and G.J. Small, *Chem. Phys. Lett.* 102 (1983) 272.
- [13] A.A. Gorokhovskii, V. Korrovits, V.V. Palm and M. Trummel, *Chem. Phys.*

- Lett. 125 (1986) 355.
- [14] R. Jankowiak and H. Bässler, Chem. Phys. Lett. 125 (1986) 139.
- [15] W. Breinl, J. Friedrich and D. Haarer, Phys. Rev. B 34 (1986) 7271.
- [16] L.W. Molenkamp and D.A. Wiersma, J. Chem. Phys. 83 (1985) 1.
- [17] C.A. Walsh, M. Berg, L.R. Narasimhan and M.D. Fayer, Chem. Phys. Lett. 130 (1986) 6; J. Chem. Phys. 86 (1987) 77.
- [18] M. Berg, C.A. Walsh, L.R. Narasimhan, K.A. Littau and M.D. Fayer, Chem. Phys. Lett. 139 (1987) 66.
- [19] J. Fünfschilling and I. Zachokke-Gränacher, Chem. Phys. Lett. 110 (1984) 315.
- [20] B. Jackson and R. Silbey, Chem. Phys. Lett. 99 (1983) 331.
- [21] H.P.H. Thijssen, thesis, University of Leyden (1985), p. 37 and references therein.
- [22] H.M. van Noort, thesis, University of Leyden (1981), chapter 3.
- [23] S. Völker, R.M. Macfarlane, A. Genack, H.P. Trommsdorff and J.H. van der Waals, J. Chem. Phys. 67 (1977) 1759.
- [24] R. van den Berg and S. Völker, to be published.
- [25] J. Friedrich and D. Haarer, Angewandte Chemie, 23 (1984) 113.
- [26] H. de Vries and D.A. Wiersma, J. Chem. Phys. 72 (1980) 1851.
- [27] P.J. van der Zaag, J.P. Galaup and S. Völker, to be published.

$i = \text{overlapping}$
 $q = \text{major}$

ACKNOWLEDGEMENTS

This report is the end of one and a half years work at the MAT. In this period I learned many things from many people and I wish to express my gratitude to my co-workers.

In the first place there is Rob, who taught me the experimental techniques, and to apply them in the most efficient manner. All my ingenious ideas he laughed away. I want to thank Hans for not laughing at my ideas, but trying to oppose them until the end. Pieter-Jan always backed me up by a short résumé of the situation and his opinion. I am indebted to Silvia, with whom I worked through the spectra, and who always saw things in these spectra that I had overseen. And last but not least all the people who made this place a place where it is a pleasure to work.

I am grateful to all the people who corrected the text of this report for me, especially Rob and Silvia, who worked until late in the night on it. Rob assisted me in the measurements and let me use some of his data. Bert, Prof. Schmidt, Richard and Marian guided me through the word-processing system. To all,